1988

Processing of 2090 aluminum alloy for superplasticity.

Regis, Henry C.

NAVAL POSTGRADUATE SCHOOL
Monterey, California

THESIS

PROCESSING OF 2090 ALUMINUM ALLOY FOR SUPERPLASTICITY

by

Henry C. Regis

June 1988

Thesis Co-Advisors: T. R. McNelley
S. J. Hales

Approved for public release; distribution is unlimited.

REPORT DOCUMENTATION PAGE

. REPORT SECURITY CLASSIFICATION NCLASSIFIED	1b RESTRICTIVE MARKINGS
. SECURITY CLASSIFICATION AUTHORITY	3 DISTRIBUTION / AVAILABILITY OF REPORT Approved for public release, distribution is unlimited.
. DECLASSIFICATION / DOWNGRADING SCHEDULE	
PERFORMING ORGANIZATION REPORT NUMBER(S)	5 MONITORING ORGANIZATION REPORT NUMBER(S)
NAME OF PERFORMING ORGANIZATION aval Postgraduate School 6b OFFICE SYMBOL (If applicable) Code 69	7a NAME OF MONITORING ORGANIZATION Naval Postgraduate School
ADDRESS (City, State, and ZIP Code) onterey, California 93943-5000	7b. ADDRESS (City, State, and ZIP Code) Monterey, California 93943-5000
NAME OF FUNDING / SPONSORING ORGANIZATION 8b OFFICE SYMBOL (If applicable)	9 PROCUREMENT INSTRUMENT IDENTIFICATION NUMBER
ADDRESS (City, State, and ZIP Code)	10 SOURCE OF FUNDING NUMBERS PROGRAM ELEMENT NO / PROJECT NO / TASK NO / WORK UNIT ACCESSION NO

. TITLE (Include Security Classification)
rocessing of 2090 Aluminum Alloy for Superplasticity

. PERSONAL AUTHOR(S)

a. TYPE OF REPORT	13b TIME COVERED	14 DATE OF REPORT (Year, Month, Day)	15 PAGE COUNT
aster's Thesis	FROM _____ TO _____	1988, June	71

. SUPPLEMENTARY NOTATION
he views expressed in this thesis are those of the author and do not reflect the official olicy or position of the Department of Defense or the U. S. Government.

COSATI CODES		
FIELD	GROUP	SUB-GROUP

18 SUBJECT TERMS (Continue on reverse if necessary and identify by block number)
Aluminim-Copper-Lithium Alloys 2090, Thermomechanically Processing, Superplasticity

. ABSTRACT (Continue on reverse if necessary and identify by block number)

The applicability of a thermomechanical process, involving warm rolling to facilitate ontinuous recrystallization (CRX), to aluminum alloy 2090 was considered. The thermo-echanical process has been shown to result in 2-5mm grains and superplasticity at 300°C in l-Mg and Al-Mg-Li alloys. In this study, the warm rolling temperature and the reheating ime between consecutive rolling passes were varied. Superplastic ductility of 320 percent as obtained during tesion testing at 350°C. Microstructural analysis of the structures roduced during warm rolling indicates inadequate interaction between precipitating phases nd dislocation structures. Thus, improved warm-temperature superplastic ductility may be btained by initial precipitation treatments followed by warm rolling.

DISTRIBUTION / AVAILABILITY OF ABSTRACT ☒ UNCLASSIFIED/UNLIMITED ☐ SAME AS RPT ☐ DTIC USERS	21 ABSTRACT SECURITY CLASSIFICATION UNCLASSIFIED
a NAME OF RESPONSIBLE INDIVIDUAL rofessor T. R. McNelley	22b TELEPHONE (Include Area Code) (408)646-2589 22c OFFICE SYMBOL 69Mc

) FORM 1473, 84 MAR 83 APR edition may be used until exhausted
All other editions are obsolete

SECURITY CLASSIFICATION OF THIS PAGE

☆ U.S. Government Printing Office 1986—606-243

UNCLASSIFIED

Approved for public release; distribution is unlimited.

Processing of 2090 Aluminum Alloy for Superplasticity

by

Henry C. Regis
Lieutenant, United States Navy
B.S.M.E., Auburn University, 1980

Submitted in partial fulfillment of the
requirements for the degree of

MASTER OF SCIENCE IN MECHANICAL ENGINEERING

from the

NAVAL POSTGRADUATE SCHOOL
June 1988

ABSTRACT

The applicability of a thermomechanical process, involving warm rolling to facilitate continuous recrystallization (CRX), to aluminum alloy 2090 was considered. The thermomechanical process has been shown to result in 2–5 mm grains and superplasticity at 300° C in Al-Mg and Al-Mg-Li alloys. In this study, the warm rolling temperature and the reheating time between consecutive rolling passes were varied. Superplastic ductility of 320 percent was obtained during tension testing at 350° C. Microstructural analysis of the structures produced during warm rolling indicates inadequate interaction between precipitating phases and dislocation structures. Thus, improved warm-temperature superplastic ductility may be obtained by initial precipitation treatments followed by warm rolling.

TABLE OF CONTENTS

LIST OF FIGURES

I. INTRODUCTION

Superplastic behavior has now been extensively documented in Al-Mg alloys, with elongations in excess of 1,000 percent obtained in many cases in these alloys. The applications for aluminum alloys capable of deforming superplastically are numerous and superplastic forming has been shown to be economically viable, particularly when the production run of a part falls in a certain range of units. Superplastic forming (SPF) processes are currently being used in the production of airframe components for aerospace vehicles such as the B1-B bomber, the F-15 Eagle, and the F/A-18 fighter/attack aircraft. Eliminating the use of fasteners, and therefore local areas of stress concentration, is a very desirable feature of the manufacture of single-piece components by superplastic forming. The introduction by Alcoa of an Al-Li alloy called Alithalite, or 2090, whose composition is registered with the Aluminum Association, reflects the interest the aluminum industry has in developing an alloy with good potential for superplastic forming as well as high strength-to-weight ratio, favorable ductility and toughness, and good high-cycle fatigue characteristics.

The aviation industry especially has already adopted the use of superplastic forming for various airplane components where weight reductions and the ability to form complex shapes in one piece are crucial. Characteristics of superplastic behavior include a fine grain size (two to five microns), a strain rate sensitivity coefficient $m > 0.3$,

and deformation at temperatures > 0.5 Tm. A material is considered to exhibit a superplastic response when elongations of at least 200 percent are obtained prior to failure in tension. In this work, elongations up to 320 percent were obtained at a test temperature of 350° C. This alloy also weighs seven to eight percent less and demonstrates ten percent higher stiffness than 7075 aluminum, an alloy it was designed to replace. This is due to the presence in the alloy of lithium, which produces a relatively great reduction in density per unit added.

The intent of this study is to determine the effect of higher isothermal rolling temperatures and longer (up to 30 minutes) reheating times between rolling passes on the thermomechanical processing of this alloy, with the purpose of obtaining superplasticity at lower temperatures than is currently the case. Tensile testing temperatures were also increased in comparison to previous research done on this alloy [Ref. 1]. Knowledge gained from previous work on the thermomechanical processing (TMP) of Al-Mg-Li-Zr alloys was applied to 2090, an Al-Cu-Li-Zr alloy, with the intention of obtaining a fine, evenly distributed second-phase precipitate and a fine grain size by thermomechanical processing (TMP).

II. BACKGROUND

A. ALITHALITE ALLOY 2090

Alithalite alloy 2090 is produced commercially by Alcoa and the composition is now registered with the Aluminum Association. As previously mentioned, it is an Al-Cu-Li-Zr alloy and is intended to replace the 7075 alloy widely used in the aeronautical industry today. The 2090 alloy has good mechanical properties when fully aged. Cold working prior to aging raises the ultimate tensile strength to about 500 MN/m^2. Corrosion resistance compares favorably with other high-strength alloys [Ref. 2].

It also has seven percent lower density and ten percent higher elastic modulus when compared to 7075 alloy [Ref.1]. Although the details of the processing of 2090 are proprietary, it is known that the alloy is cold worked by stretching and then heat treated. The purpose of the stretch is to introduce a dislocation structure to provide sites for precipitation, which in turn give the material enhanced combinations of strength and toughness. The final wrought product is available in sheets, plates, extrusions in a T8 temper condition, or forgings in a T6E203 condition [Ref.1].

B. SUPERPLASTICITY

Superplasticity is the ability of a metal to experience large tensile elongations without localized necking. Elongations as high as 1,000 percent have been obtained in aluminum, while normal alloys exhibit

ductilities of 100 percent or less. Nothing more than a laboratory curiosity a few years ago, superplastic forming is now considered an economical method to manufacture complex structures in one piece, therefore avoiding stress concentrations at rivets or other attachments. The aircraft industry especially has seized the opportunity to fabricate components by superplastic forming. Parts made by the Northrop corporation for the F/A-18 Hornet strike fighter use this technology to reduce the number of parts required as well as cut cost by up to 30 percent [Ref.3]. This section of the background will introduce to the reader methods to achieve superplasticity in aluminum alloys and the mechanisms which are thought to be associated with it.

1. Phenomenological Considerations

In order to facilitate superplastic forming, the following characteristics for a material must be obtained through processing:

1. A fine, equiaxed grain size.
2. The presence of a uniformly distributed second phase precipitate.
3. Resistance of the material to cavitation.

Relatively low strain rates (10^{-2} to 10^{-4} sec^{-1}) applied during forming are also required, as is deformation at a temperature T= 0.5 T_m, where T_m is the melting temperature. The strain rate is critical during superplastic forming due to its effect on the strength of any material capable of achieving superplasticity. The flow stress, σ, increases rapidly with the strain rate $\dot{\varepsilon}$ [Ref. 4], as seen in the equation:

$$\sigma = K\dot{\varepsilon}^{m}$$

where m is the strain rate sensitivity exponent and K is a material constant. Values of m are obtained from experimental data by applying the equation:

$$m = \frac{d \ln \sigma}{d \ln \dot{\varepsilon}}$$

It has been shown experimentally that the elongation prior to failure is directly related to the value of m (elongation increases as m increases). A value of m of approximately 0.5 provides the high elongations with strain rates varying between 10^{-4} and 10^{-2} sec^{-1}. A low value of m in association with necking of a test sample results in a local strain rate increase, while a high value of m causes a slower increase in the strain rate at the neck [Ref.4].

It is generally accepted that a fine grain size is required to achieve superplasticity, due to the dependence of strain rate on grain size [Ref. 4]:

$$\dot{\varepsilon} = Kd^{-2} \qquad (1)$$

What mechanism in the microstructure brings about a superplastic response? It is generally accepted that grain boundary sliding, accommodated by dislocation motion near the boundaries, is the principle mechanism taking place allowing such deformations. Sherby and Wadsworth [Ref. 4] have described this phenomenon with the relation:

$$\dot{\varepsilon} = \frac{A \cdot D_{eff}}{d^2} \left(\frac{\sigma}{E}\right)^2 \qquad (2)$$

where A= 6x 10^9, $\dot{\varepsilon}_{spd}$ is the strain rate during SPD, d is the grain size, and E is Young's modulus. D^*_{eff} is a modified diffusion coefficient given by [Ref. 5]:

$$D^*_{eff} = D_l + \frac{\pi c \delta}{d} D_{gb}$$

where c= 0.01, D_{gb} is the grain boundary diffusion coefficient, δ is the thickness of a grain boundary layer, and D_l is the lattice diffusion coefficient. Equations (1) and (2) suggest that the superplastic response of a metal will be enhanced by refinement of the grain size.

2. Microstructural Considerations

Sherby and Wadsworth [Ref. 4] discuss typical grain sizes of ten microns or less in diameter, while McNelley and Hales [Ref. 5] point to an optimum grain size of 2 to 5 microns for a wrought Al-10Mg-0.1Zr alloy. The presence of a uniformly distributed second phase is also considered beneficial by inhibiting grain growth, as long as the second phase precipitates size remains fine and its distribution uniform. More specifically, the presence in small quantities of the element zirconium prevents grain growth during recrystallization of a heavily rolled alloy [Ref. 4]. The Zirconium intermetallic is extremely fine and slow to coarsen—two traits highly desirable for microstructural stability at superplastic deformation (SPD) temperatures [Ref. 6]. Grain shape should be equiaxed after thermomechanical processing and should vary little in shape during SPD [Ref. 5].

Two processing routes can be utilized to induce superplastic behavior in Al-Li alloys: the "Rockwell" processing route and the "Supral" processing route. The "Rockwell" method involves producing a fully recrystallized fine grain structure prior to SPD, while in the "Supral" method both recrystallization and a fine grain size are obtained during the formation operation. This latter method is normally employed with Al-Cu alloys and is similar to the thermomechanical processing used in this work and previous work at Naval Postgraduate School.

C. RECRYSTALLIZATION

1. Recovery

Recovery is the process by which a tangled network of dislocations is rearranged to a lower energy configuration with a reduction in residual stresses in the material. By this process, dislocations are rearranged into a polygonized structure. The driving force for the recovery is the strain energy previously stored in the alloy via cold work or other deformation process. The polygonized structure which results is a subgrain structure now using the rearranged dislocations as subgrain boundaries.

The high stacking fault energy (SFE) associated with aluminum (166mj/m^2 for pure aluminum) signifies that dislocations will readily recover by cross slip and climb [Ref. 7]. The addition of Cu and Li lowers the SFE somewhat, but the alloy still maintains a relatively high stacking fault energy. The significance of this is that

metals with a high stacking fault energy will produce well-defined cell structures when strained [Ref. 8].

Dynamic recovery also occurs during the rolling (hot working) process. Dynamic recovery is also associated with metals with a high SFE such as aluminum [Ref. 9].

2. Discontinuous Recrystallization (DRX)

Discontinuous recrystallization (DRX) is the process initiated by nucleation and followed by growth of new strain free grains occurs along a well-defined reaction front. Nucleation has been observed to take place at particle-matrix interfaces, or at least within the "deformation zone" surrounding a particle [Ref. 10].

The greater the deformation imparted to a material, the more likely recrystallization will occur as a result of the increased number of nucleation sites. The nucleation and growth of new, recrystallized grains is closely related to the distribution of dislocations in the rolled alloy [Ref. 8].

Small strains during rolling will provide few nucleation sites, which in turn will result in a coarse structure when combined with a high rate of growth. In contrast, if a large amount of deformation is imparted to the material during rolling, the number of nucleation sites will increase, leading to a fine structure, even with a relatively high rate of growth.

Second-phase particles represent nucleation sites for discontinuous recrystallization in aluminum [Ref. 11]. Thus, precipitate size and spacing are critical for the control of grain size during DRX. This

and spacing are critical for the control of grain size during DRX. This is also true for continuous recrystallization (CRX) [Ref. 12]. DRX occurs by high-angle boundary migration as a means for lowering the stored energy due to deformation. Thus, a different texture is formed compared to the surrounding deformed microstructure [Ref. 9].

3. Continuous Recrystallization

The continuous recrystallization mechanism (CRX) has been much debated in recent years, but no one model has yet been widely accepted. The most notable aspect of CRX is the absence of a recrystallization front, associated with nucleation and high-angle boundary migration as in DRX [Ref. 7]. CRX occurs by subgrain formation and coalescence wherein groups of dislocations situated in low angle boundaries react to form boundaries of greater misorientation. Essentially, dislocations are being rearranged to form energetically more favorable configurations in this "advanced recovery" mechanism. The degree of refinement attainable and the misorientation resulting in grain boundaries would be expected to depend on the dislocation density, that is, the amount of straining that has been done on the material. It has been recognized in previous studies by Wise and Salama [Refs. 13 and 14] that the total true strain during rolling does influence the resulting superplastic response and, therefore, based on these studies, a total strain during rolling of 2.5 was selected. This strain corresponds to a reduction in area of 92 percent.

The CRX mechanism is initiated with formation of nuclei by the coalescence of subgrains into one larger subgrain. However, this

uniform growth of subgrains, involving coalescence reactions, follows and gradually converts a structure containing low angle boundaries to one consisting of moderate angle boundaries of misorientation on the order of five to seven degrees [Ref. 5]. The texture of the material remains essentially the same. The mechanism is generally thought to involve a combined recrystallization-precipitation process, itself favored by a high density of nucleation sites, although the role of the precipitates is not entirely clear.

In aluminum alloys or other high stacking fault energy materials, these sites are more than likely subgrain boundary junctions [Ref. 9]. Second-phase precipitates and the spacing between them play a significant role in the rate of subgrain growth as well. Also, analysis of subgrain formation during creep reveals that an increase in the applied stress leads to a decrease in subgrain size [Ref. 12].

This in turn seems to indicate that an increase in dislocation density (reflected in an increase in subboundary misorientation angle) by TMP will induce greater misorientations in the resultant boundaries of the microstructure, and thus improve the SPD properties of the alloy [Ref. 15].

Nes [Ref. 16] proposes a model for CRX in Zr-bearing aluminum alloys due to a strain-induced continuous reaction. First, the requirement exists for a high density of fine dispersoids to retard high-angle boundary migration. Zirconium additions in particular are unique in producing very fine dispersion of small Al_3Zr particles. According to Nes [Ref. 16], during the hot deformation process for

Supral (Al-CuZr) alloys, subgrain boundaries migrate and the stabilizing Al_3Zr particles go partially into solution due to grain boundary migration by diffusion. Later, the Al_3Zr reprecipitates and distributes itself to the larger, more stable Al_3Zr particles which survived the grain boundary migration effect.

Nes [Ref. 16] also explains the rapid increase in boundary misorientation which occurs with CRX by the subgrain coalescence phenomenon, reinforced by grain boundary sliding associated with random grain rotations. Continuous recrystallization allows the formation of a more refined microstructure than does discontinuous recrystallization.

The reader may question whether these equations devised by Sherby and Wadsworth [Ref. 4] are applicable to microstructures exhibiting grain boundary misorientations of approximately five to seven degrees. Nes [Ref.16] concluded that boundary sliding in such a structure is possible and Salama [Ref 14] reached a similar conclusion regarding the behavior of Al-Mg alloys.

D. PREVIOUS INVESTIGATIONS AT NPS

Previous work at the Naval Postgraduate School on 2090 aluminum alloy was performed by Spiropoulos [Ref. 1]. This work centered on finding a thermomechanical processing method, including warm rolling, to produce a fine grain microstructure and thus enhance superplasticity. The intention was for the 2090 alloy to undergo microstructural changes via the CRX mechanism, similar to what had been seen with Al-Mg-Li-Zr alloys in previous studies [Refs. 13 and 14].

The thermomechanical process is initiated with the homogenization of the material by solution treatment, 10 percent cold working, followed by a low-temperature aging treatment to allow initiation of homogeneous precipitation. The subsequent isothermal warm rolling was performed at 300° C in a manner promoting continuous recrystallization in the metal. Warm rolling was conducted isothermally by reheating the alloy between rolling passes and reheating intervals of either 4-minute or 30-minute duration were utilized to facilitate recovery and CRX during the rolling. Elevated temperature testing was then performed to assess the effect on ductility. Microscopy results did indicate a more uniform distribution of second phase using a 30-minute reheating time, but ductility data indicated that the extent was insufficient for CRX.

Spiropoulos [Ref. 1] proposed that the microstructure evolved by a continuous reaction, with the reaction being dependent on diffusion and thus exponentially temperature dependent. Hence, reheating temperature as well as time should effect the extent of CRX.

Transmission Electron Microscopy (TEM) work conducted in Spiropoulos's [Ref. 1] research showed no evidence of CRX, with instead a subgrain structure only. This was true for TMPs using reheating times of both 4 and 30 minutes, with rolling done at 300° C. It was also postulated from the TEM that the second phase had not precipitated and coarsened enough to interact with the recovering substructure sufficiently to stabilize it and allow CRX to occur.

E. OBJECTIVE OF THIS RESEARCH

The purpose of this thesis is to extend the previous work by Spiropoulos [Ref. 1] on 2090 alloy, in an attempt to determine processing conditions leading to CRX. This, in turn, would be expected to extend downward the temperatures at which superplastic forming may be done and would result in formed material of finer structure and lessened cavitation damage.

III. EXPERIMENTAL PROCEDURE

A. MATERIAL

The alloy 2090-t8A41 studied in this thesis was fabricated by ALCOA. The dimensions of the material as received were about 51 x 31 x 4 cm (L x W x T). The material was heat treated to a T8 temper (solution heat treated, cold worked, and then artificially aged) [Ref. 17] and anodically coated in a A41 type of coating (architectural class I) [Ref. 18].

Previous work [Ref. 1] had shown that the chemical composition of this alloy in weight percent (ANAMET Laboratories Inc., Berkeley, California [Ref 19]) is as follows in Table 1:

TABLE 1

SAMPLE COMPOSITION

	Cu	Li	Zr
1	2.52	2.01	0.12
2	2.60	2.03	0.12
3	2.56	2.04	0.12
Average	2.56	2.03	0.12
Nominal	2.70	2.20	0.12

B. PROCESSING

1. Solution Treatment and Upset Forging

Billets of dimensions of about 41 x 43 x 51 mm had previously been sectioned from the plate. Billets were solution treated at 540° C for two hours. Solution treatment was conducted to dissolve the soluble precipitates in the alloy. The solvus temperature for Cu alone is 450° C and for Li alone 400° C. Solution treatment was performed at 540° C, well above those solvus temperatures. The temperature was closely monitored by a thermocouple located in the center of the furnace and close to the billet. The billets were then upset forged between two platens continuously heated at 480° C, re-solution treated at 540° C for a period of one hour, followed by a quench into 10° C water. Each heated platen temperature was monitored by thermocouples, as was the temperature in between the two platens just prior to the upset forging process. The purpose of the hot work process is to further refine and homogenize the alloy after the solution treatment process. The billets were upset forged along their longest dimension (parallel to the subsequent rolling direction of the plate), from an initial dimension of 50.8 mm to about 25.4 mm. The cold water quench was utilized to avoid any precipitation during cooling.

2. Thermomechanical Processing

a. Cold Working

The thermomechanical process consisted of an initial ten-percent cold working followed by warm rolling. Each forged billet, sectioned into two pieces, was reduced from an initial thickness of

25.4 mm to a final thickness of 22.9 mm to achieve the desired cold work. The purpose of the cold working is to introduce dislocations which provide nucleation sites as the phases precipitate. No age treatment was conducted between cold rolling and warm rolling processes as no significant improvement was obtained previously from aging [Ref. 1]. Figure 3-1 is a schematic illustration of the basic thermomechanical processing used.

b. Warm Rolling

In order to study the effects of higher rolling temperatures on the mechanical properties of this alloy, and considering a warm working temperature range between 200° C and the solvus of 2090 [Ref. 20], oven temperatures of 350°, 400°, and 450° C were utilized between rolling passes. Table 2 shows the various TMPs used :

TABLE 2

THERMOMECHANICAL PROCESSING SCHEDULE

TMP Temperature	Reheating Time Between Passes (min)	Total Rolling Strain	Reduction Per Pass (mm)
350	4	2.5	2.5
350	30	2.5	2.5
400	4	2.5	2.5
400	30	2.5	2.5
450	4	2.5	2.5
450	30	2.5	2.5

All billets were pre-heated for 30 minutes to the desired temperature of each warm rolling process prior to that process. Four and thirty-minute reheating times were used between each rolling

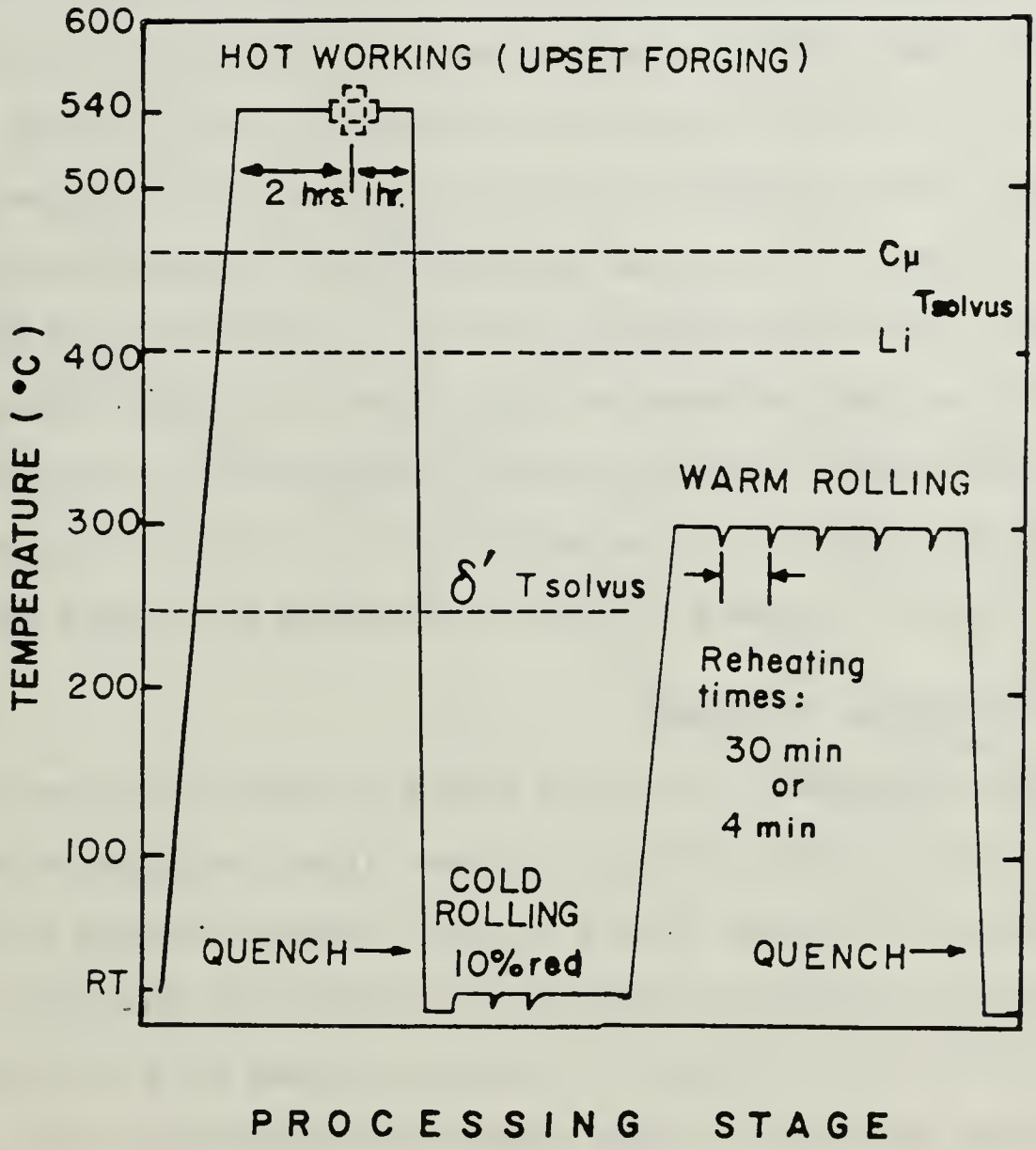

Figure 3-1. **Thermomechanical Processing Techniques**

pass for every rolling temperature utilized. To ensure a total true strain of approximately 2.5 (± 0.1) for each rolling process and in order to avoid a sample too thick prior to the final pass, an initial reduction of five percent was used for each first pass through the rollers. This was followed by ten-percent reductions per pass until the final rolling pass, which was approximately a five percent reduction as well (in order not to exceed the overall true strain desired). This technique, devised by Kuhnert [Ref. 21], proved to be the best processing technique to obtain an appropriate sample dimension for the final pass, while still submitting the alloy to the desired ten-percent reductions per pass and an overall true strain of 2.5. A preheating time of 30 minutes was chosen as previous research [Ref. 1] demonstrated that excessive preheating (one hour) prior to initiating warm rolling resulted in severe cracking of the billet during the first rolling pass.

C. MECHANICAL TESTING

Upon completion of the warm rolling process, final sheet thicknesses varied between 1.35 and 1.80 mm. These variations were due to variation in the upset forging process. Specimen blanks were cut out from the rolled sheets to the dimensions given by Wise [Ref. 13:p. 31] and illustrated in Figure 3-2. Testing samples were cut with the longitudinal dimension of the sample corresponding to the prior rolling direction. A Marshall Model 2232 three-zone clamshell furnace mounted on an Instron tensile testing machine was used to perform the required high-temperature testing. Tensile testing was conducted in accordance with Table 3.2.

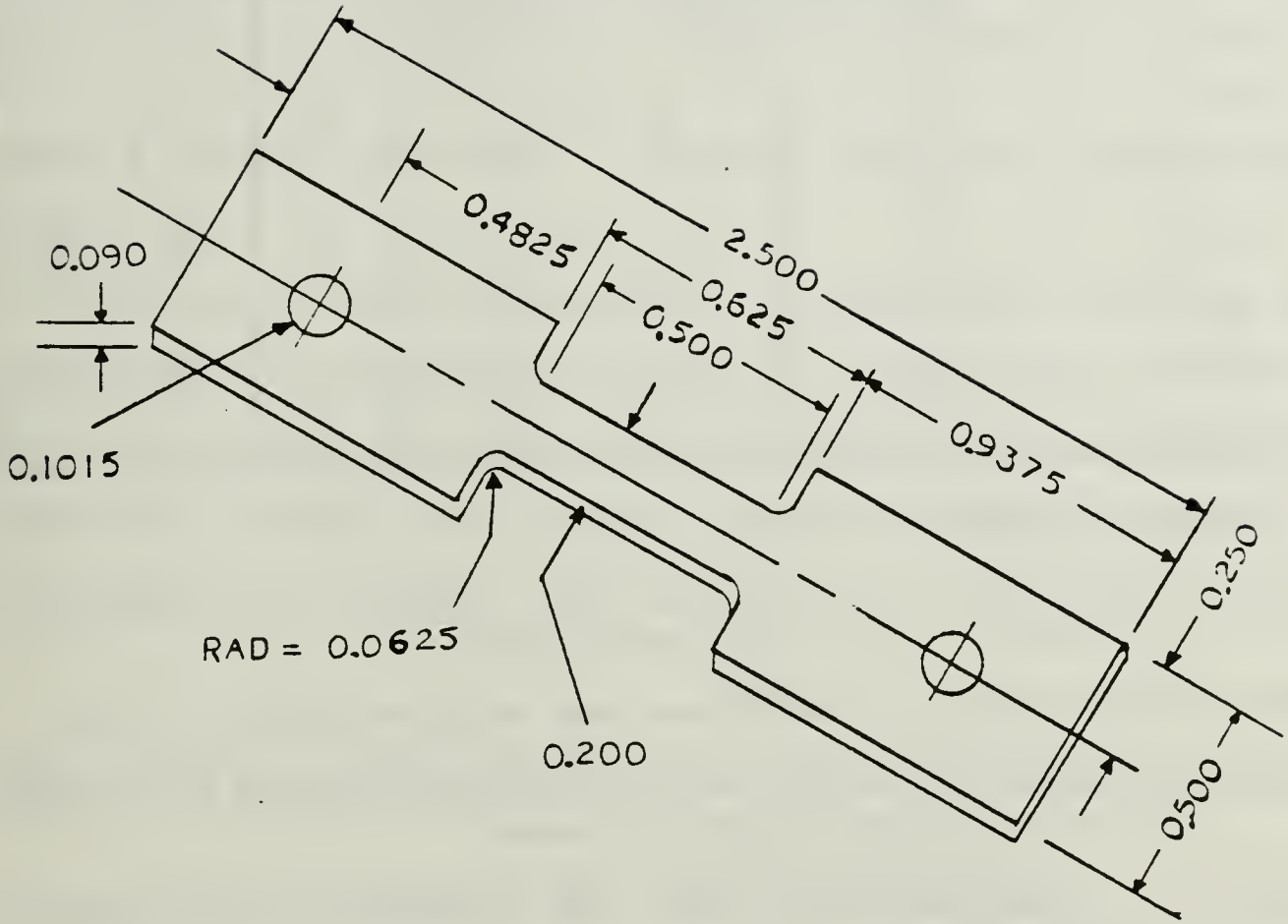

Figure 3-2. **Test Specimen Dimensions**

TABLE 3

PROCESSING CONDITIONS WITH APPLIED TESTING TEMPERATURES

Tensile Testing Temperatures	Rolling Temperatures with 4 and 30 min. Reheating							
	300° C		350° C		400° C		450° C	
	4 m/p	30 m/p	4 m/p	30 m/p	4 m/p	30 m/p	4 m/p	30 m/p
300° C	X*	X*	X	X	X	X	X	X
350° C				X		X	X	
370° C*	X	X						
400°C			X	X	X	X	X	X
440° C*	X	X						
450° C			X		X		X	
510° C	X	X						

* Previous work [Ref. 1]

Note 1: Reduction per pass was kept constant (approximately 2.5 mm)

Note 2: Final rolling true strain was kept at approximately 2.5 (±0.1)

Note 3: Some of the previous work includes aging, which had negligible effect on the properties obtained.

Note 4:
- Tensile testing at 300° C was performed for five different strain rates.
- Tensile testing at 350° C and higher was performed for only two strain rates: 6.67×10^{-3} and $6.67 \times 10^{-4} s^{-1}$.

Crosshead speeds were selected to yield the desired strain rates. Load versus time data were autographically recorded and converted to true stress versus true strain curves via the following data reduction process.

Actual elongation was measured by taking the difference between the measured gage section prior to testing and the final length measured after failure of the sample. Percent elongation was calculated as follows:

$$\% \text{ elongation} = \frac{(L_f - L_0)}{L_0} \times 100$$

where L_0 is the initial length of the gage section and L_f is the final length.

Factors such as grip slippage and the elastic deformation of the sample were accounted for by the use of a "floating slope" to convert data from the strip chart and calculate strain and corresponding stress values. Data reduction was performed using the following formulas:

$$\text{Magnification ratio} = \frac{c}{x}$$

where x is the crosshead speed and c is the chart speed;

$$\text{Correction Factor} = \frac{\text{Actual elongation}}{\text{Measured elongation}}$$

where measured elongation is the horizontal distance between the "floating slope" and the zero load point, all divided by the magnification ratio (a scale factor). The actual elongation is simply L_f - L_0.

$$\text{Engineering strain } e = \frac{(L_f - L_0)}{L_0}$$

$$\text{True strain } \varepsilon = \ln(1 + e)$$

$$\text{Engineering stress } S = \frac{P}{A_0}$$

$$\text{True stress } \sigma = S(1 + e)$$

All reduced data was obtained through the use of a simple Fortran language computer program included in Appendix A. An Easyplot program, available with the Naval Postgraduate School IBM 3033 computer, was utilized for all graphic and figures generated.

D. METALOGRAPHY

Optical microscopy (OM) was carried out to study the effects of the thermomechanical processing on the microstructure of 2090 aluminum alloy. Specimens were taken from the as-rolled condition for the following TMPs: 450° C rolling combined with either 4- or 30-minute reheating per pass (the highest elongation was achieved with the first process). Both rolling and transverse surfaces of the as-rolled samples were examined.

Cold mounting of the specimens was accomplished by using an acrylic compound. Wetted silicon carbide abrasive papers were used for polishing following a sequence of 240, 320, 400, and 600 grit. Final polishing was accomplished using a diamond paste and then magnesium oxide. Etching was performed using Keller's etchant for 8 to 14 seconds. A Zeiss ICM 405 optical microscope was used for the microscopic examination.

IV. RESULTS AND DISCUSSION

Microstructural data were obtained in this research for a limited range of processing conditions. These are compared to the data reported by Spiropoulos [Ref. 1] and extend the previous work. Tensile testing was then accomplished over a range of temperatures to study the effect of prior processing on the subsequent deformation properties. Results again were compared with those of Spiropoulos [Ref. 1] to extend the range of work on this alloy.

A. EFFECTS OF PROCESSING ON MICROSTRUCTURE

1. Previous Results

Spiropoulos [Ref. 1] demonstrated clearly that increasing the reheating time between consecutive passes during rolling at 300° C resulted in a more homogeneous distribution of the second-phase precipitate particles. This was true for all process variants examined. From the TEM results, all the variants demonstrated, at best, a recovered structure, with little evidence of formation of precipitates at subboundary nodes. Based on the work of Salama [Ref. 14] on Al-Mg alloys, it is believed that the precipitation of second-phase particles at subboundary nodes stabilizes the structure during warm rolling, and the precipitate-substructure interaction thus facilitates the mechanisms which lead to CRX.

In Spiropoulos' work [Ref. 1], TEM work revealed a well-distributed precipitate for the TMP including 30-minute reheating, but

the intermetallic phase which had precipitated was quite fine and therefore had not interacted in the desired manner with the dislocation structure.

2. Optical Microscopy of This Research (As-Rolled Condition)

In this work, the extreme end of the processing regime was investigated (i.e., 450° C rolling for both 4- and 30-minute reheating times) for the material in the as-rolled condition. A relatively coarser structure was evident here (Figures 4.1 through 4.3) compared to Spiropoulos's research [Ref. 1], especially with the 30-minute reheating interval. A homogeneous distribution of second-phase particles is again evident with the TMP utilizing a 30-minute reheating time. However, this is accompanied by a much coarser second-phase particle size. If CRX is occurring, one would expect a relatively coarse structure here. It is believed that for the 450° C rolling at the longer reheating time of 30 minutes between passes, the precipitation has progressed to such an extent that the particles have significantly coarsened and, as a result, the grain structure itself is coarse. This would degrade the superplastic response of the material.

B. MECHANICAL RESULTS

1. Stress vs Strain Response

Figures 4.4 and 4.5 show typical stress-strain curves for 2090, as processed in this research employing a rolling temperature of 350° C. Data obtained at five different nominal strain rates is shown. Each curve indicates an initial hardening, followed by flow at a nearly

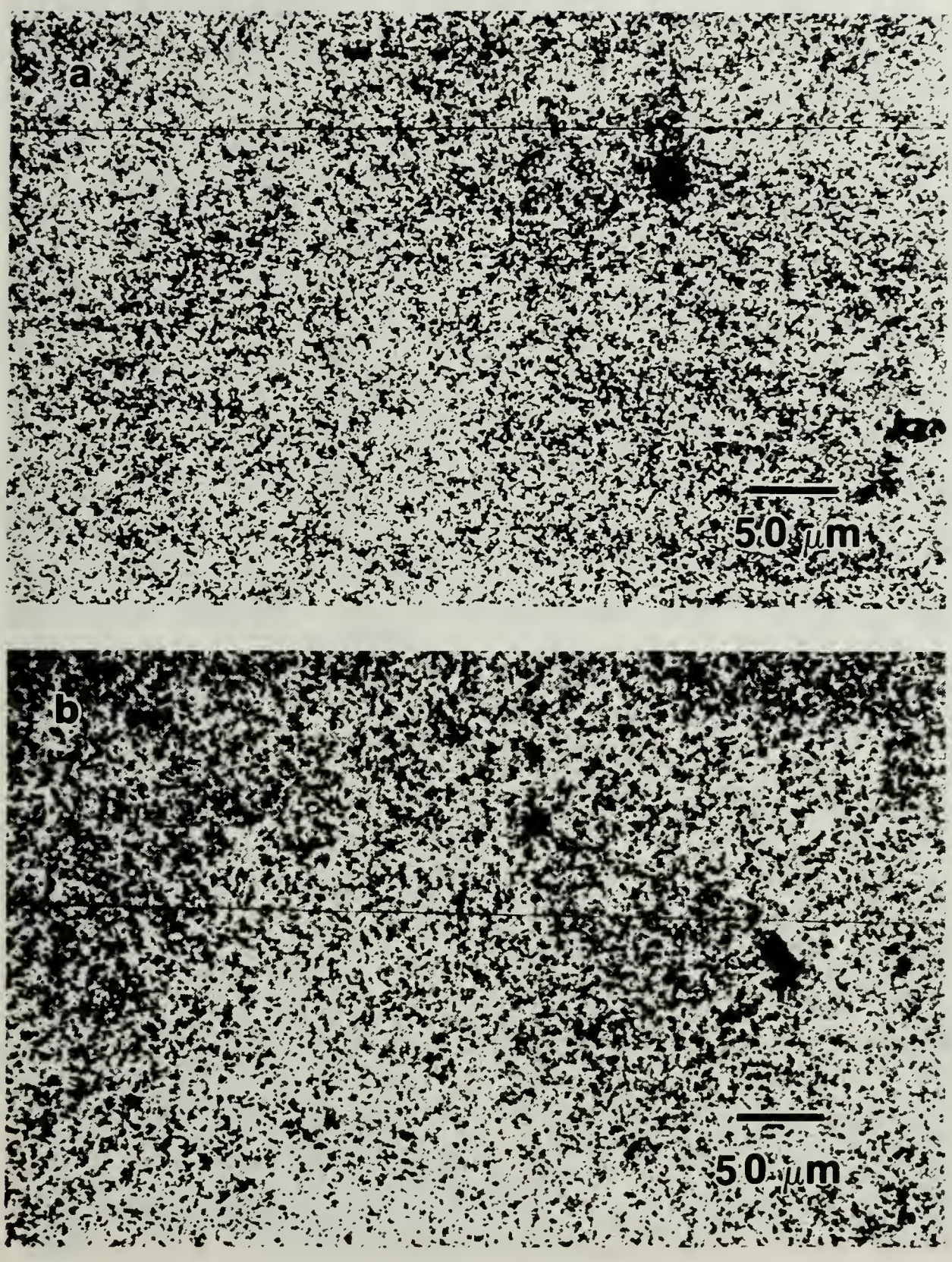

Note the coarse precipitates in (b).

Figure 4-1(a) and (b). **Optical Micrographs, Showing the Transverse Sections of As-Rolled Samples for 450° C Rolling With 4- and 30-Minute Reheating Times, Respectively**

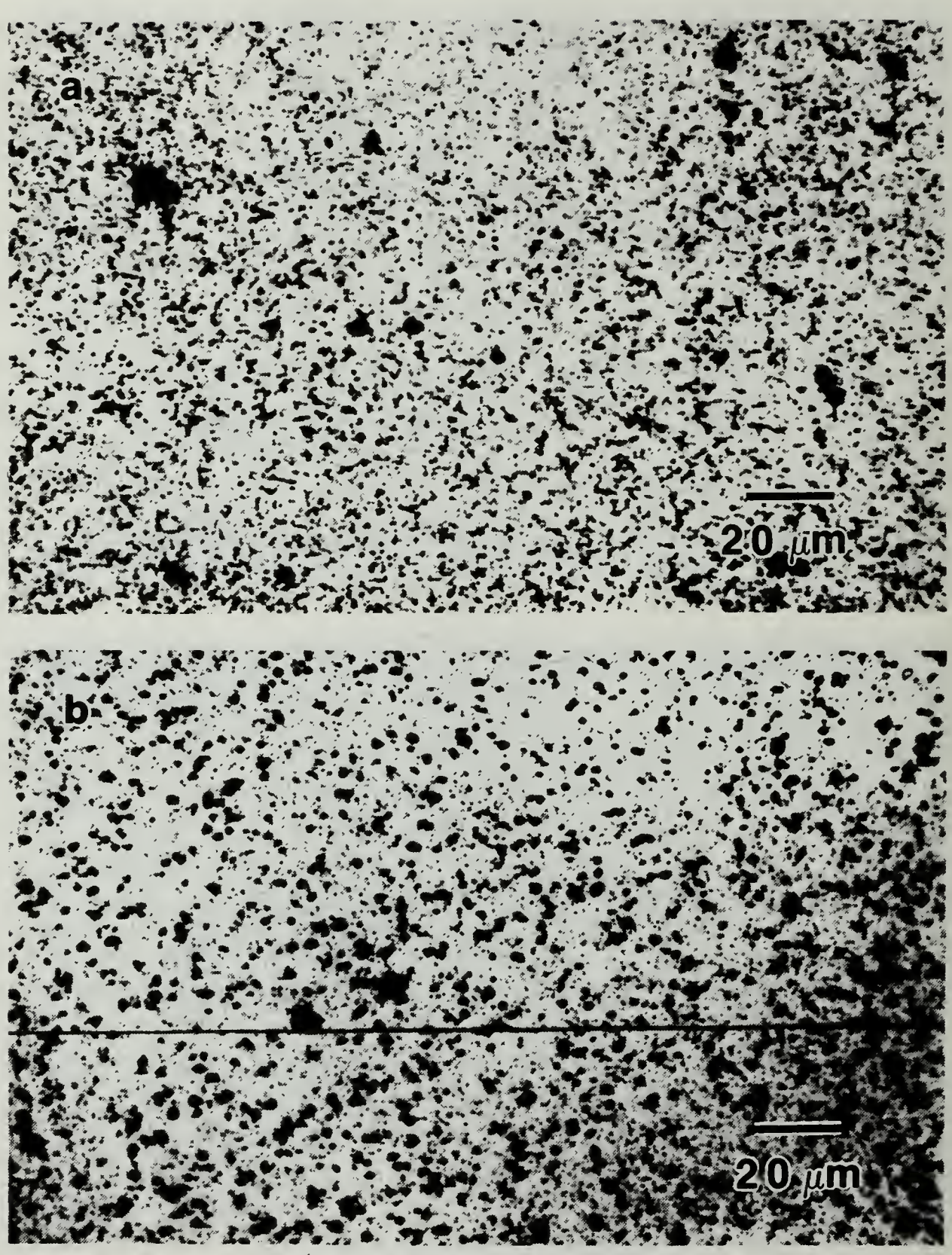

Again, note the coarser particles in (b).

Figure 4-2(a) and (b). **Optical Micrographs, Showing the Transverse Sections of As-Rolled Samples at a Higher Magnification, With 4- and 30-Minute Reheating Times, Respectively**

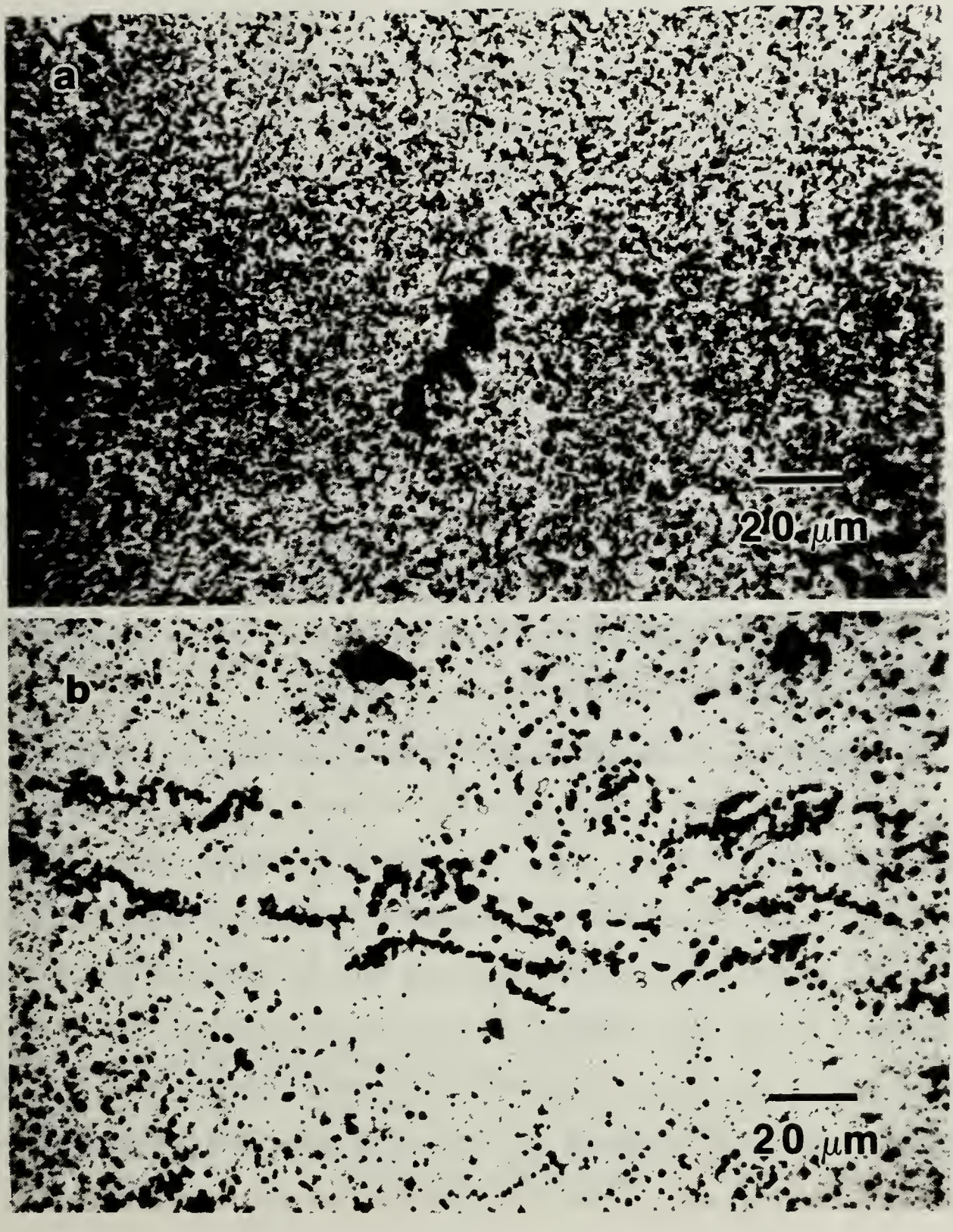

Figure 4-3(b) shows more dispersed precipitates with clear evidence of particle coarsening.

Figure 4-3(a) and (b). **Optical Micrographs, Showing the Plane of Rolling of As-Rolled Samples for 450° C Rolling at a High Magnification, With 4- and 30-Minute Reheating Times, Respectively**

constant stress value, and then concluding with a rapid decline to failure. The sensitivity of the material to strain rate is apparent, as is the increased ductility as strain rate is reduced. The curves obtained at the lowest strain rates also show more extensive flow at constant stress.

Comparison of Figures 4.4 and 4.5 clearly reveals that higher ductility values are obtained for a TMP including a 30-minute as opposed to a 4-minute reheating time for 350° C rolling and subsequent testing at 300° C. This result is essentially the same as achieved for rolling at 300° C for the same reheating times and testing temperatures [Ref. 1]. Thus, for rolling at 350° C, the longer reheating interval does seem to facilitate improved ductility.

2. Influence of Strain Rate (Testing Conducted at 300° C)

Stress vs strain rate data are shown in Figure 4-6 and 4-7, again for testing at 300° C following each of the eight different TMPs. In Figure 4-6, where all rolling involves four-minute reheating times, a significant decrease in the flow stresses and an increase in the slope m are seen as the prior rolling temperature is increased. The ductility versus strain rate data in Figure 4-8 mirrors those results, with the highest ductilities attained at the highest rolling temperatures (450° C), corresponding to the weakest condition exhibiting the largest m value.

In contrast, the data of Figures 4-7 and 4-9, illustrating the influence of rolling temperature but with the 30-minute reheating

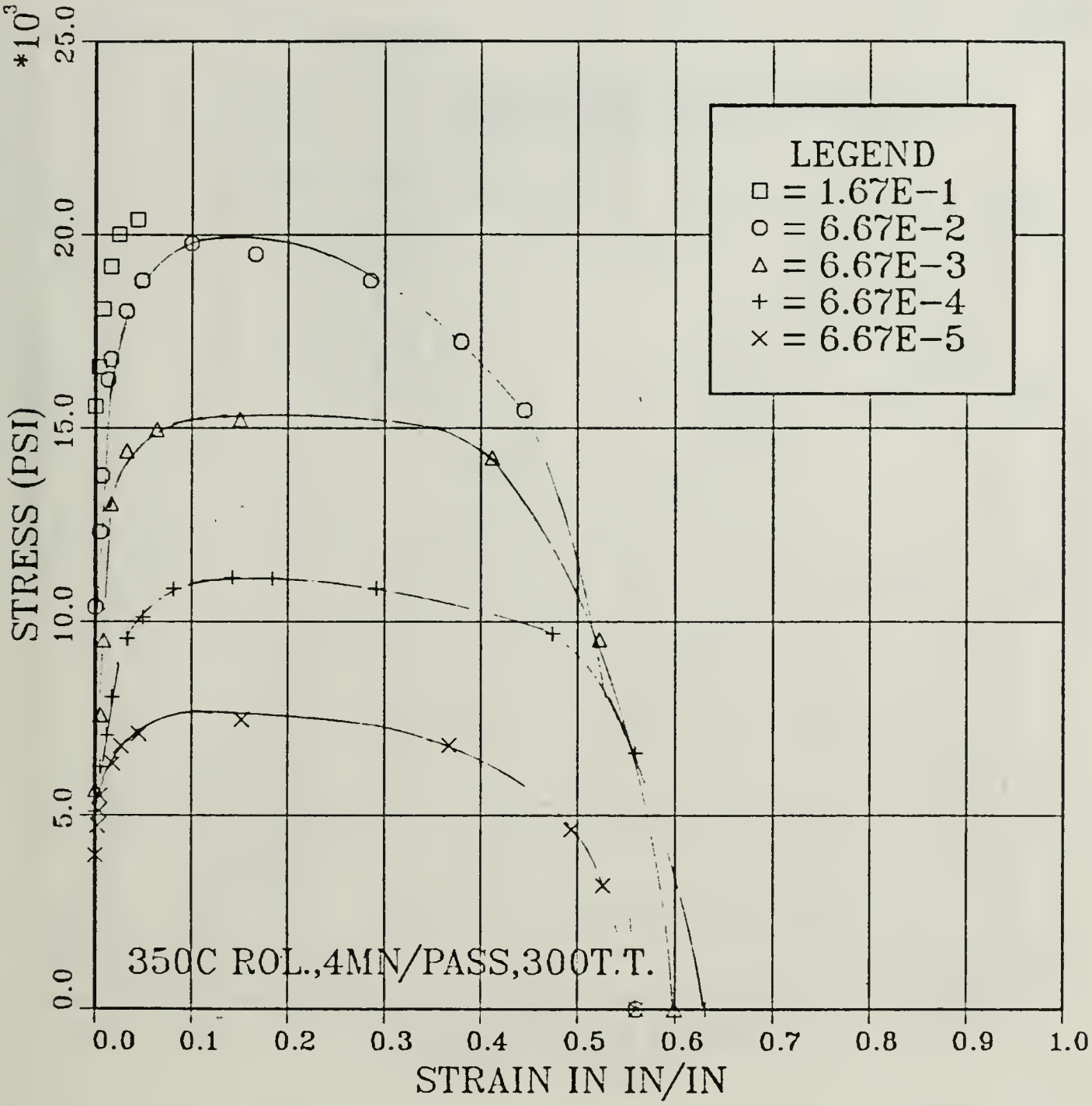

Figure 4-4. **True Stress vs. True Strain for Tensile Testing Conducted at 300° C for Material Rolled at 350° C, With 4-Minute Reheating Time Between Passes, at Various Strain Rates**

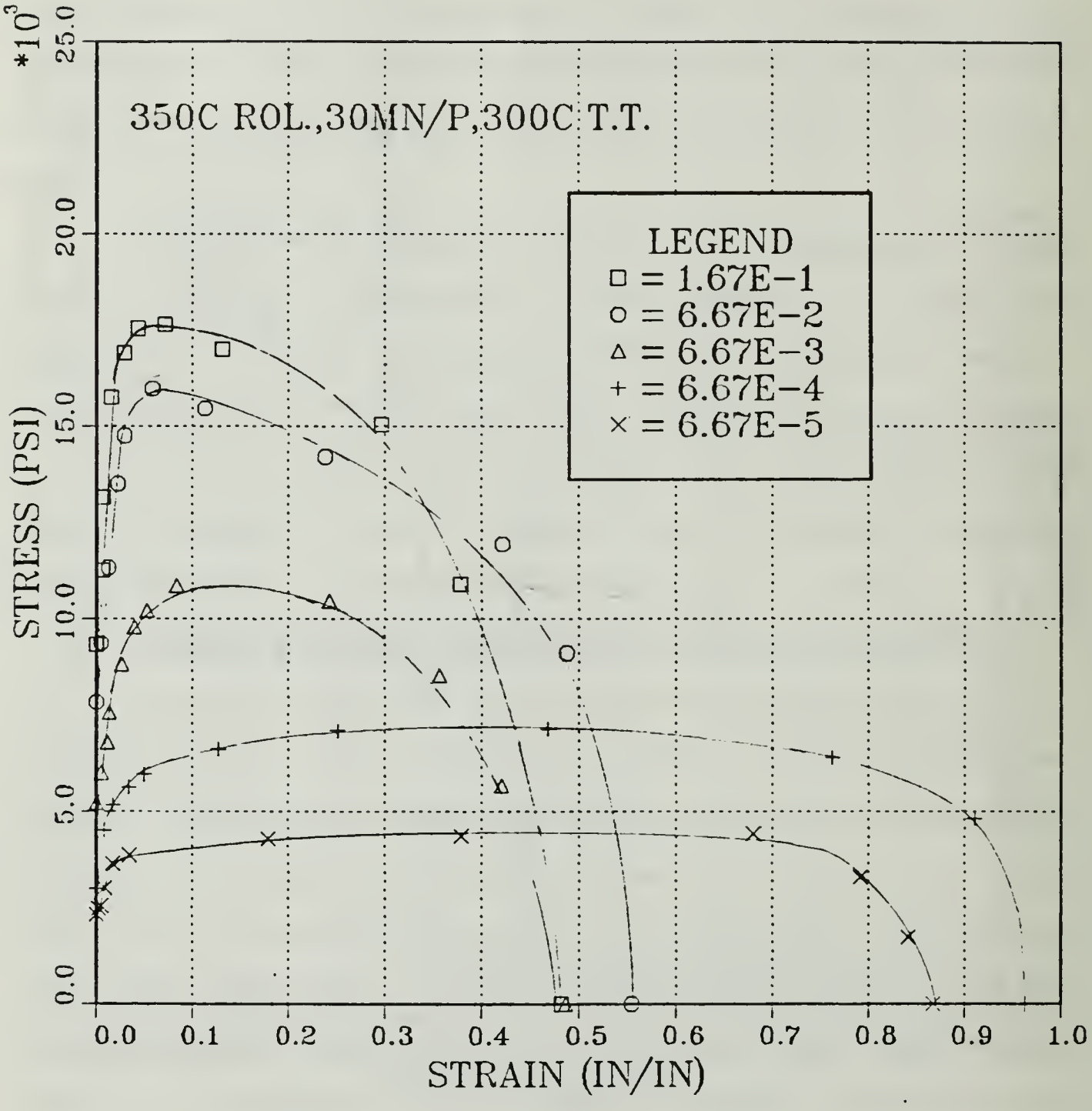

Figure 4-5. **True Stress vs. True Strain for Tensile Testing Conducted at 300° C With a 350° C Rolling, 30-Minute Reheating Time Between Passes, at Various Strain Rates**

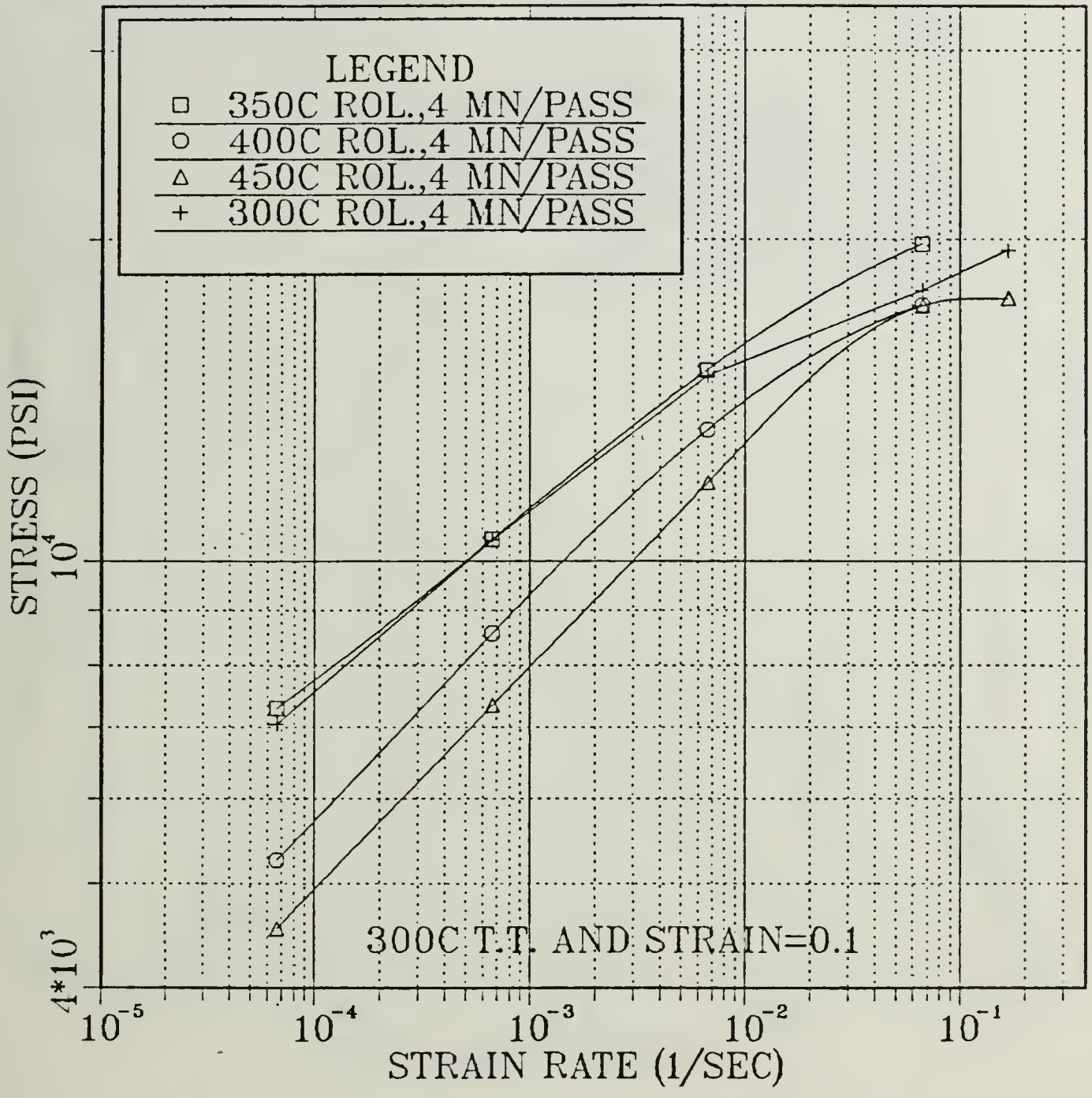

This data shows flow stress decreasing as the rolling temperature is increased, resulting in an increase in ductility with increasing rolling temperature.

Figure 4-6. **True Stress at 0.1 Strain vs. Strain Rate for Tensile Testing Conducted at 300° C for Material Processed at Temperatures Indicated With 4-Minute Reheating Time Between Rolling Passes**

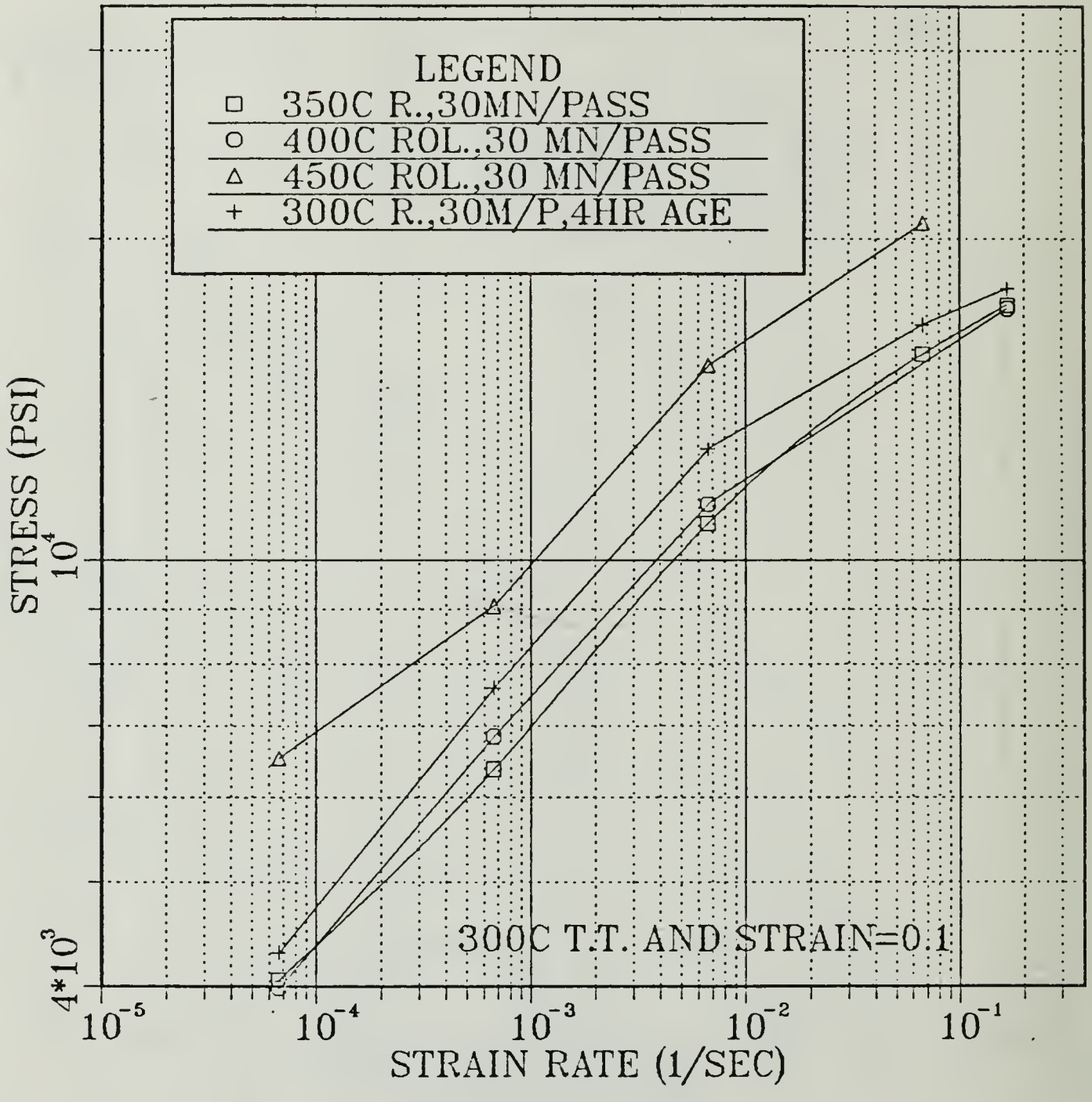

The flow stress initially goes down as the rolling temperature is increased from 350° C to 400° C, but then increases again for rolling at 400° C and 450° C.

Figure 4-7. **True Stress at 0.1 Strain vs. Strain Rate For Tensile Testing Conducted at 300° C for Material Processed With 30-Minute Reheating Time Between Rolling at Rolling Temperatures Indicated**

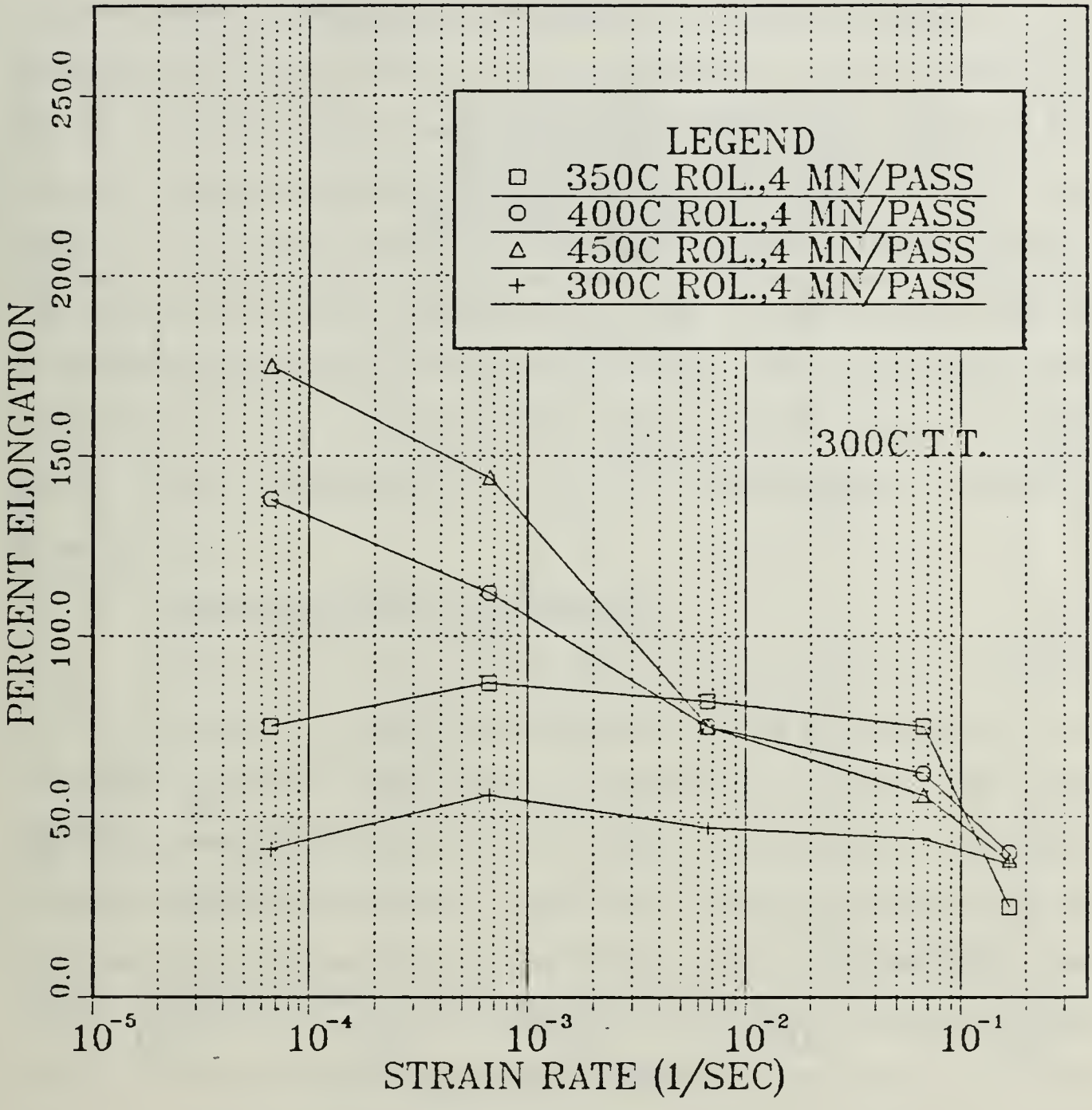

Material does show significantly higher ductilities, especially at the lower strain rates for higher temperature rolling, even though not yet in the superplastic region.

Figure 4-8. **Ductility vs. Strain Rate for Tensile Testing Conducted at 300° C for Material Processed With 4-Minute Reheating Time Between Rolling Passes**

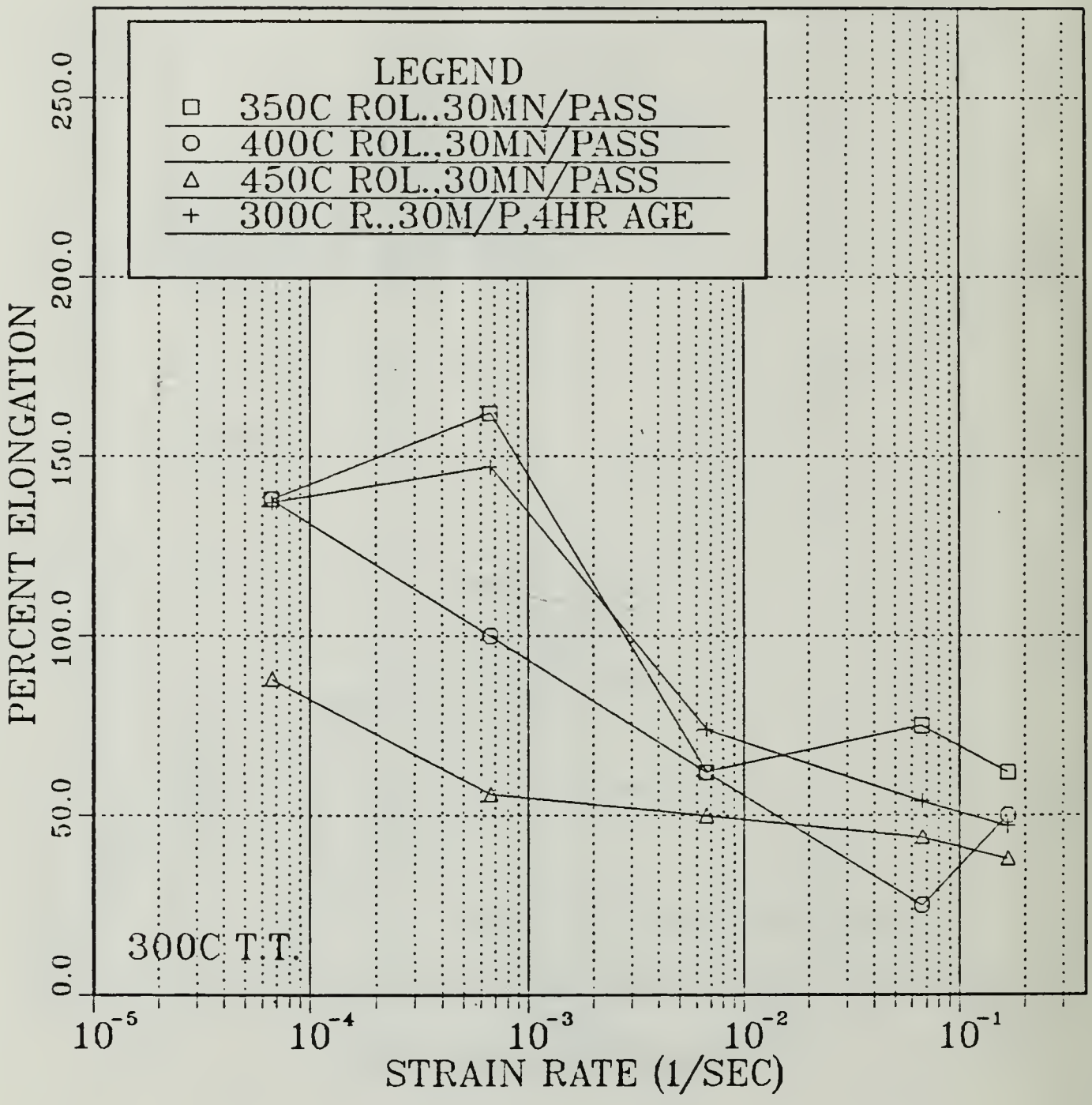

Ductilities attained with 350°, 400°, and 450° C rolling are approximately the same or lower than those achieved for 300° C rolling.

Figure 4-9. **Ductility vs. Strain Rate for Tensile Testing Conducted at 300° C for 2090 Processed With 30-Minute Reheating Times Between Rolling Passes**

time, show a decrease in flow stress for temperature increasing from 300° to 350° C, followed by increased strength at higher rolling temperatures. Again, ductility follows the behavior of the strength. The highest ductility (175 percent) was achieved for 450° C rolling utilizing four minutes between rolling passes. The next best ductility (155 percent) was obtained with the 30-minute reheating time in conjunction with a lower rolling temperature of 350° C. The last data suggest an increased grain size of the processed alloy when high rolling temperatures and long reheating times between rolling passes are combined. These characteristics are, in turn, detrimental to achieving superplasticity.

3. Influence of Test Temperature

Figures 4-10, 4-11, and 4-12 show stress (at 0.1 strain) versus strain rate for various combinations of rolling temperatures and reheating times, but now with test temperatures of 350°, 400°, and 450° C, respectively. In all cases, a decrease in flow stress as a function of testing temperature is seen. These data also demonstrate that the material is less affected by the prior warm rolling process when testing is conducted at higher temperatures. When comparing these results with previous data, no clear trend is discernable as to the effect of prior warm rolling processes, especially at the highest testing temperatures of 400° and 450° C. This is likely due to the microstructural coarsening upon heating prior to straining.

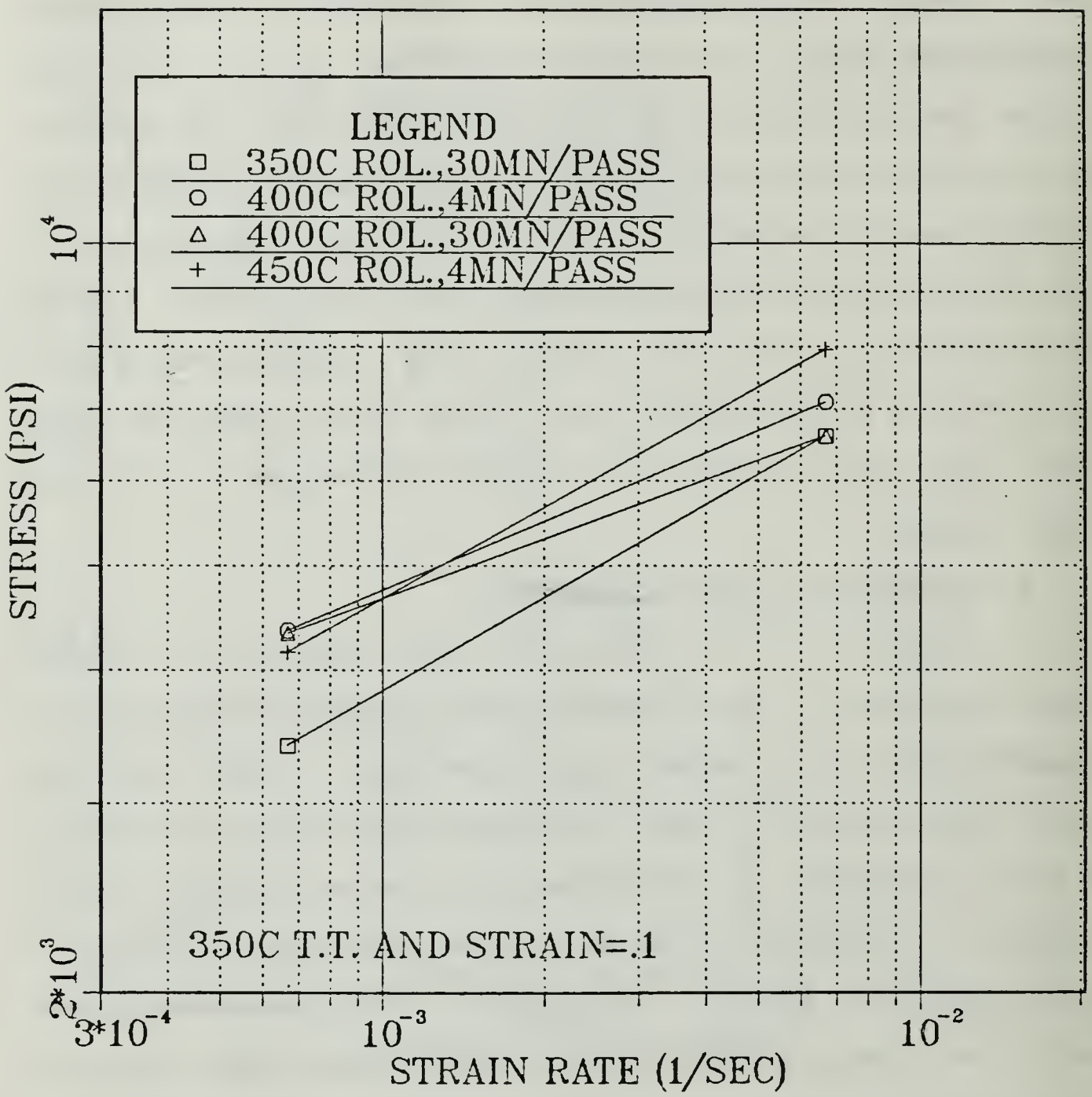

Flow stresses are lower than for material tested at 300° C but are now less affected by the prior warm rolling conditions in comparison to data obtained at 300° C.

Figure 4-10. **True Stress at 0.1 Strain vs. Strain Rate for Tensile Testing Conducted at 350° C and Material Processed as Shown in the Legend**

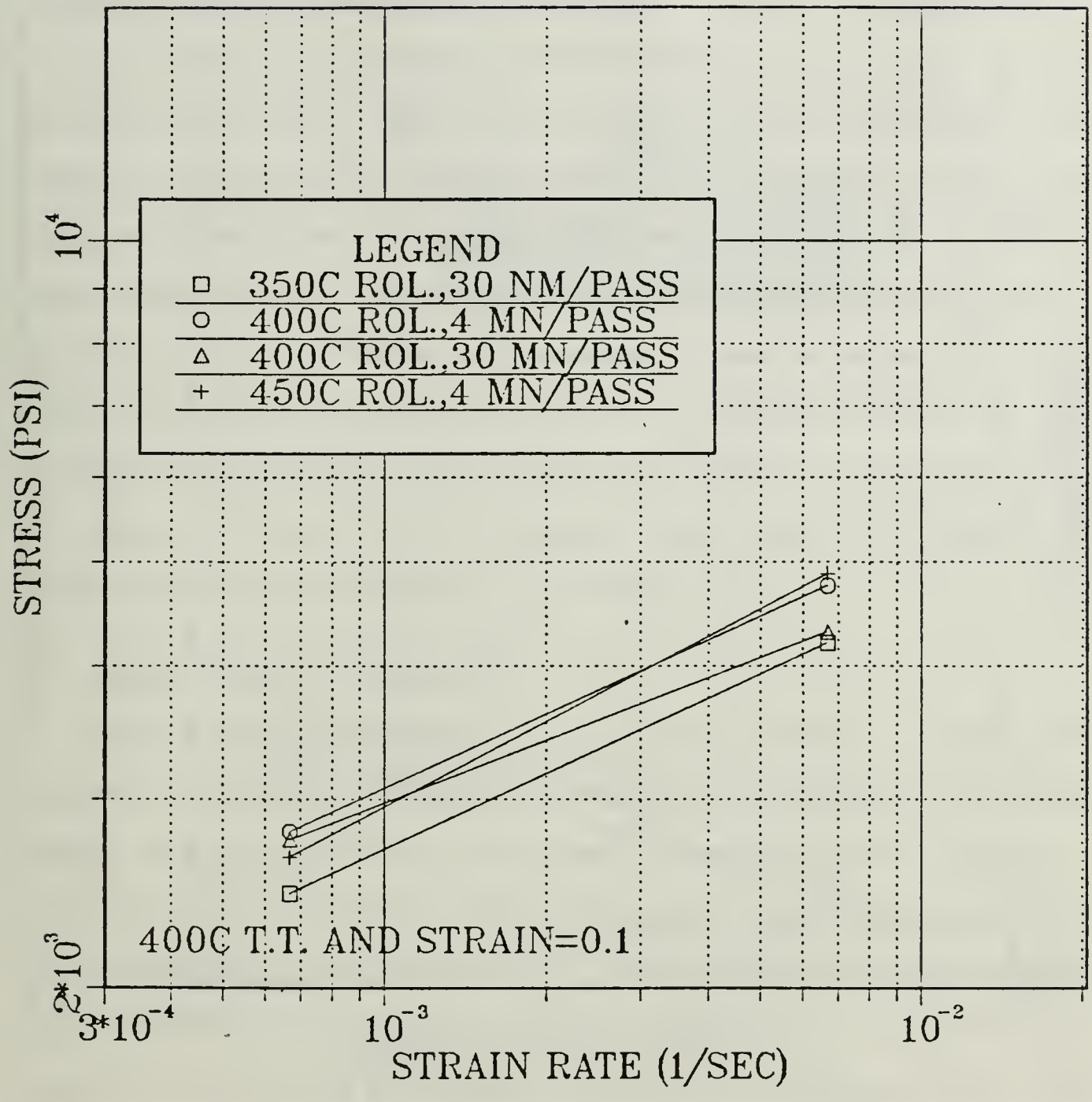

Flow stresses reached are lower than for 350° C tensile testing and are barely affected by the prior warm rolling conditions when compared to 300° C testing.

Figure 4-11. **True Stress at 0.1 Strain vs. Strain Rate for Tensile Testing Conducted at 400° C for Material Processed as Described in the Legend**

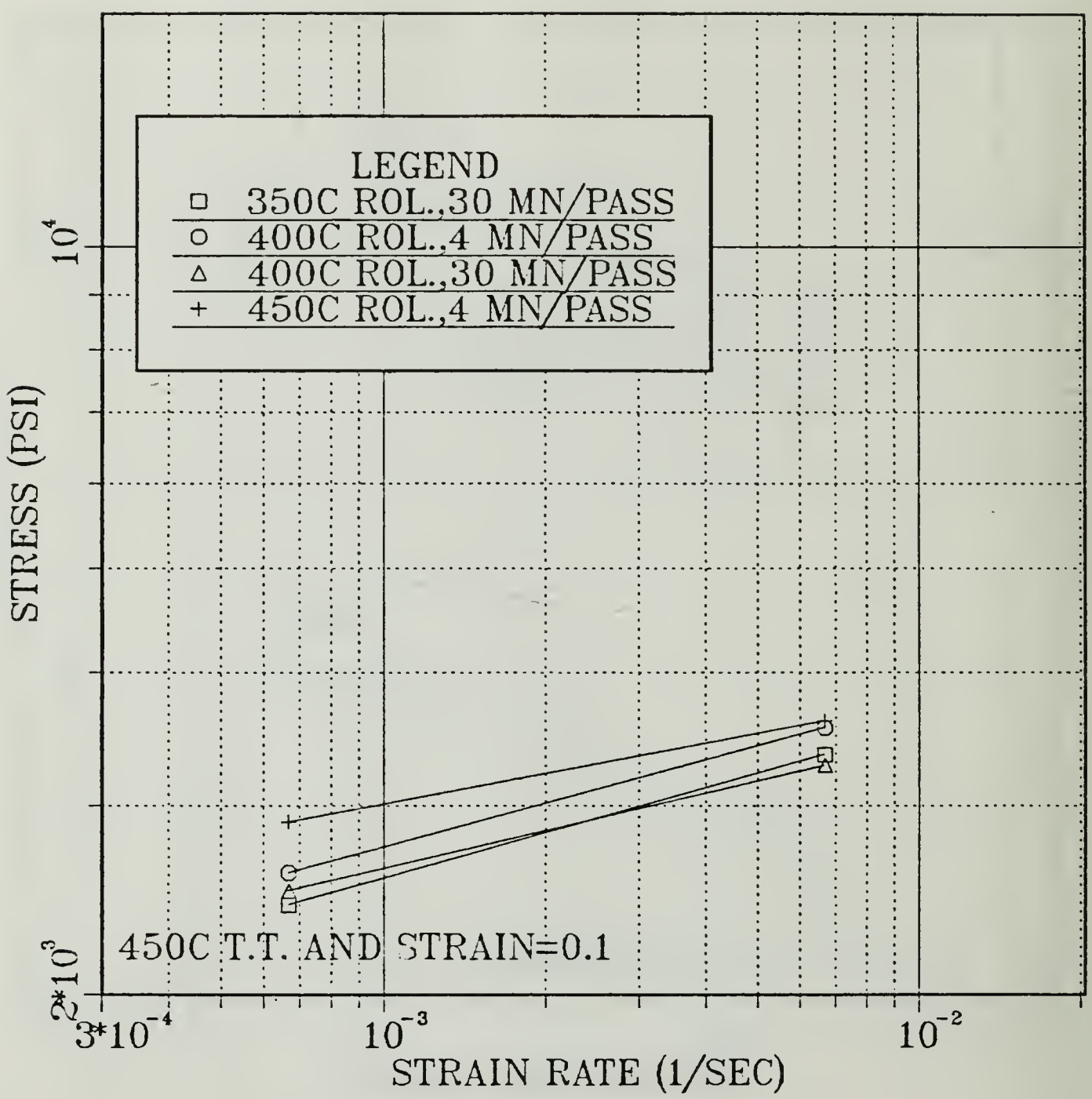

Again, flow stresses are somewhat lower than 400° C tensile testing but are less affected by the prior warm rolling temperature as compared to data obtained for 300° C testing.

Figure 4-12. **True Stress at 0.1 Strain vs. Strain Rate for Tensile Testing Conducted at 450° C**

The effects of testing temperature on ductility for testing at 6.67 x $10^{-4}s^{-1}$ strain rate are shown in Figures 4-13 and 4-14. With the four-minute reheating time utilized in the TMP (Figure 4-13), a peak in ductility is apparent at 350° C as the prior rolling temperature is increased. The highest elongation (320 percent) is achieved during 350° C testing of the material with the prior rolling accomplished at 450° C. Figure 4-14 shows similar data for rolling involving 30-minute reheating passes. The highest ductility (240 percent) was recorded for testing performed at 350° C, but the 30-minute reheating time resulted in a superplastic response (240 percent) for a lower prior rolling temperature of 350° C. The ductility data of Figures 4-13 and 4-14 correspond to the strain rate sensitivity coefficients evident in Figures 4-10 through 4-12.

C. DISCUSSION OF RESULTS

Salama [Ref. 14] observed a dramatic improvement in superplastic response of Al-Mg alloys when the reheating interval between rolling passes in the prior TMP was increased from four to 30 minutes. A model proposed by Salama [Ref. 14] suggests microstructural refinement occurs by a process of recovery of dislocations to subboundaries, resulting in increased misorientation and ultimately a microstructure capable of sustaining superplastic forming. An additional critical feature is precipitation of second-phase particles at subboundary nodes (where subgrain boundaries come together). These particles stabilize the grain boundary structure. Particles at subgrain nodes keep the dislocations from climbing apart (if they are edges); thus, as more

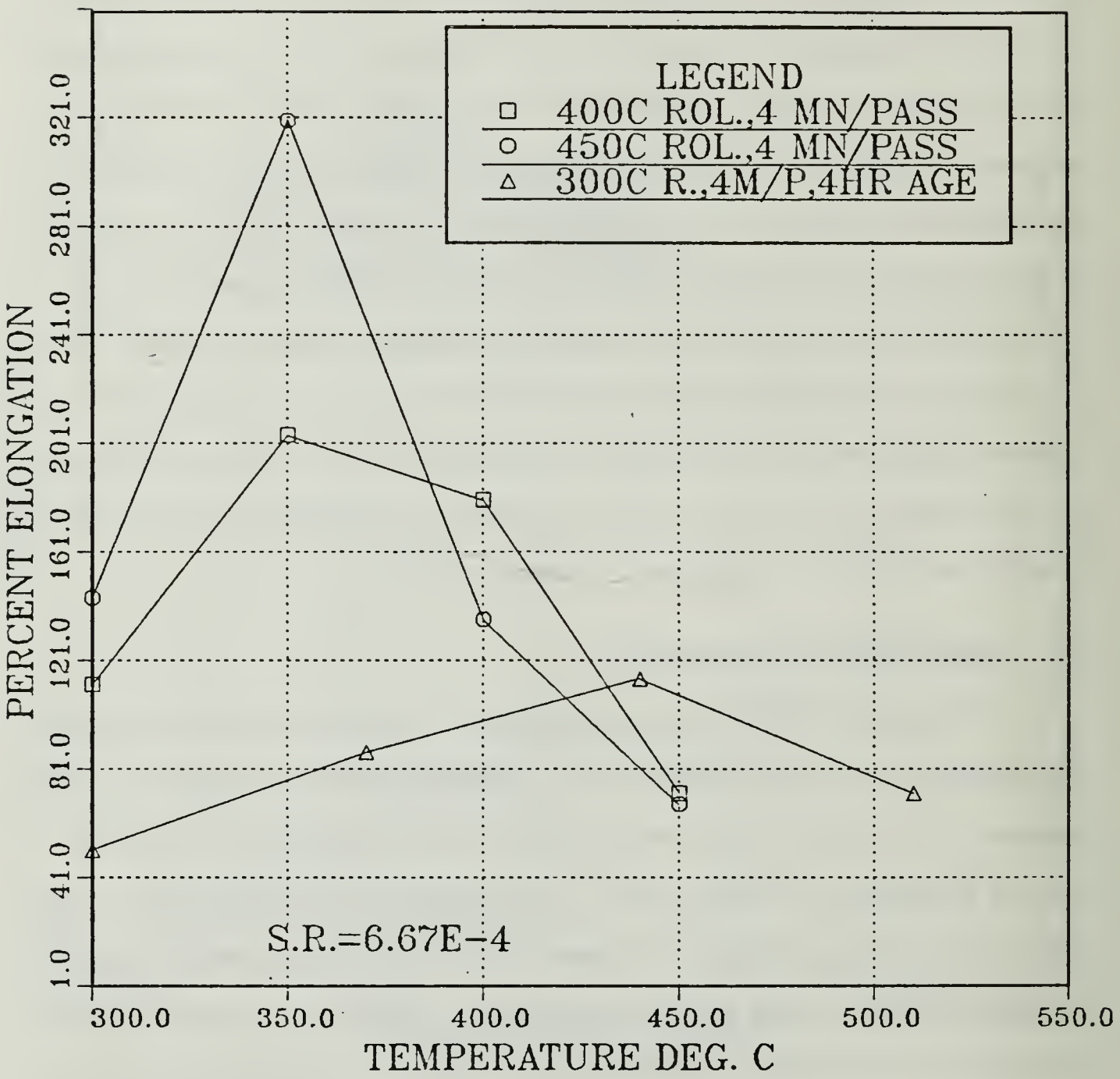

This figure illustrates the dramatic increase in ductility achieved at a testing temperature of 350° C and a rolling temperature of 450° C with 4-minute reheating time between rolling passes. In contrast, high rolling temperatures with high testing temperatures result in low ductilities.

Figure 4-13. **Ductility at 6.67 x $10^{-4}s^{-1}$ Strain Rate vs. Temperature**

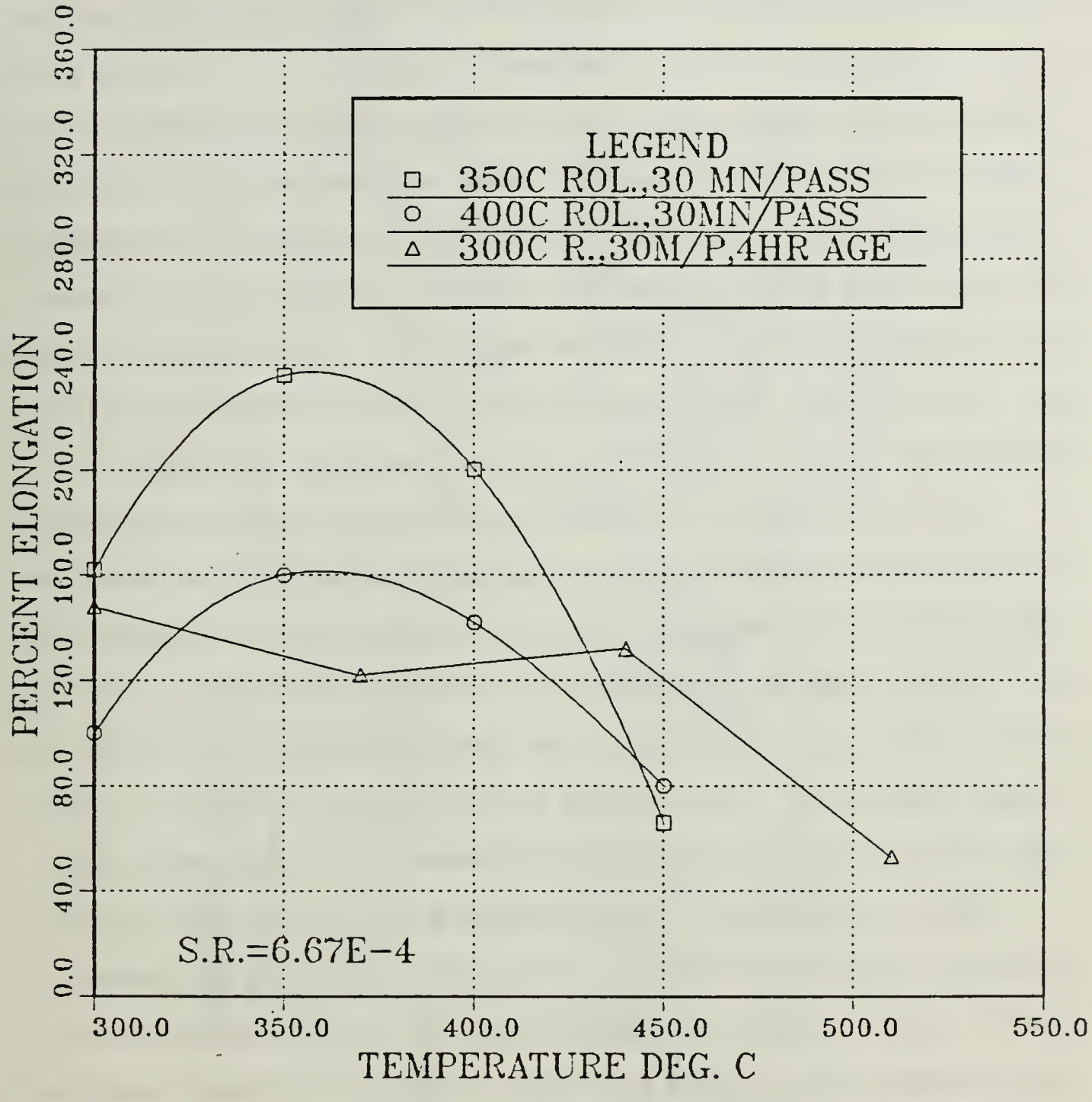

Comparison between rolling performed at 300°, 350°, and 400° C for 30-minute reheating time shows high ductilities achieved for 350° C rolling as opposed to 450° C rolling for Figure 4-7. Again, highest ductility was achieved for testing performed at 350° C. Here, a higher rolling temperature (400° C) brings about a decrease in elongation.

Figure 4-14. **Ductility at 6.67 x $10^{-4}s^{-1}$ Strain Rate vs. Temperature**

dislocations accumulate in the sub-boundary walls, the misorientations of the boundaries increase. The overall result is the formation of a moderately high-angle grain boundary over a period of rolling-recovery cycles. The model to explain these observations is illustrated schematically in Figure 4-15. Essentially, the increase in reheating interval allows sufficient time for recovery of dislocations, generated by the rolling, to recover to subboundary walls. The boundaries again are stabilized by precipitates, and thus the misorientations of the boundaries will increase as recovery to the boundary takes place.

Thus, rolling under conditions which promote both the formation of relatively high misorientation boundaries and a fine grain structure will enhance the superplastic response of the material. If the particles are too large and too far apart due to excessive coarsening, or are not present in sufficient quantity, the resulting grain size will be too coarse. Conversely, if the particles are too fine, as in Reference 1, they will not exert the desired stabilizing influence on the final grain size.

TEM work performed by Spiropoulos [Ref. 1] reveals that only smaller particles were able to precipitate for rolling performed at 300° C. Optical microscopy obtained here for 450° C. rolling reveals a more widely spaced, coarse precipitate, suggesting a coarser grain size as well (greater than 10 microns).

Data obtained in this research is consistent with the model proposed by Salama [Ref. 14] and the time-temperature correlation suggested by Spiropoulos [Ref. 1] and Kuhnert [Ref. 21]. In this work and

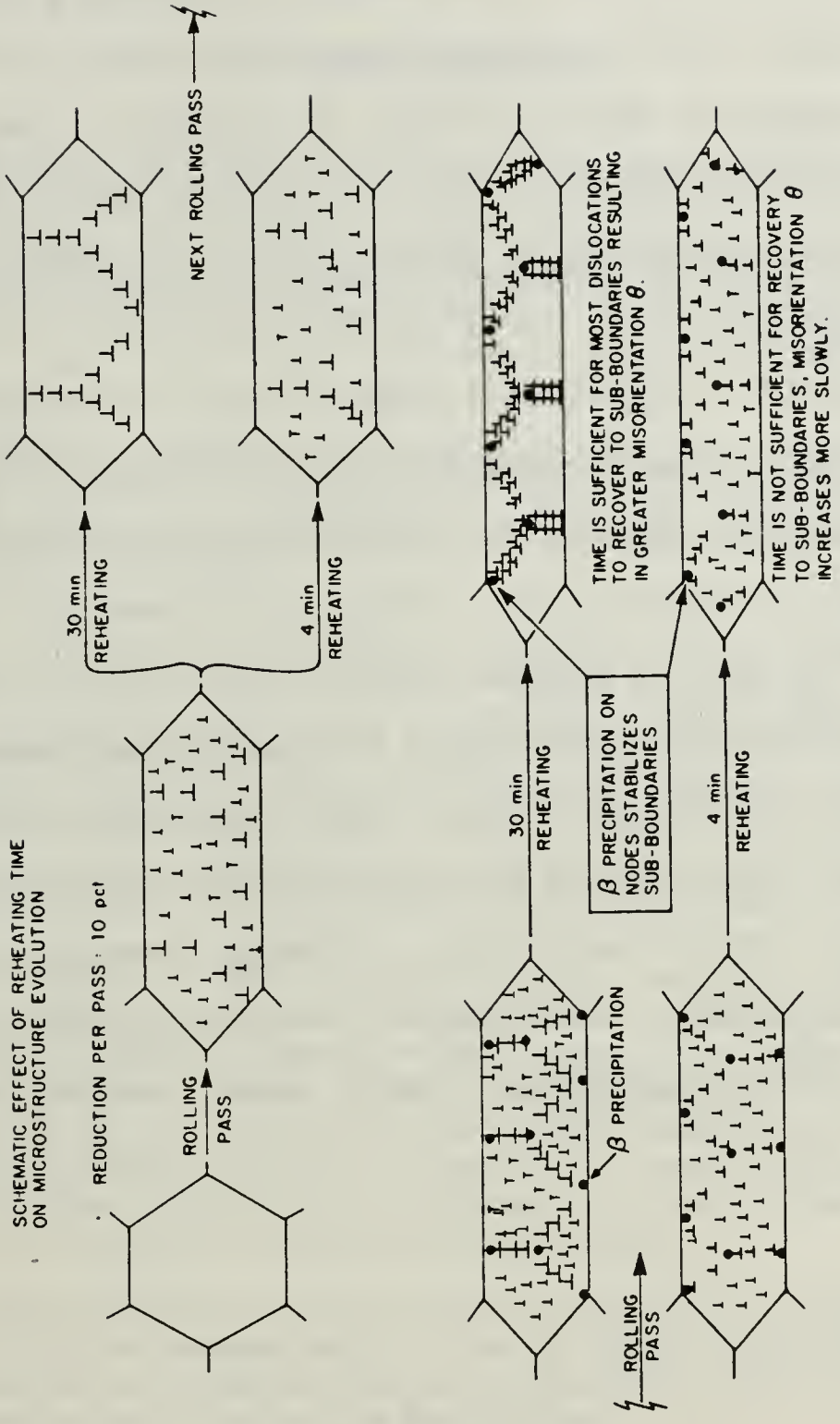

These diagrams compare structures anticipated to result from rolling with nominal reduction of 10 percent per pass and with either a short reheating interval (4 minutes) or a long reheating interval (30 minutes).

Figure 4-15. **A Schematic Representation of the Evolution of Microstructure Through a Sequence of Rolling Passes**

in Spiropoulos's work [Ref. 1], increasing the reheating time between passes resulted in an increase in subsequent ductility for the lower rolling temperatures (300° and 350° C). At higher rolling temperatures (450° C in particular), a shorter reheating time enhances the superplastic response and is necessary to avoid grain and second-phase coarsening.

Even though a superplastic response has been attained in this research (320-percent elongation), the ductilities do not correspond to those obtained in 2090 at 500° C by other approaches [Ref. 22] or to the ductilities attained via warm rolling of, for example, Al-Mg alloys [Ref. 13]. It is believed that the precipitate-sub-structure interaction did occur in this work at the higher processing temperatures, but the precipitation was followed by coarsening, resulting in coarse grains. Thus, it may be necessary in future research to separate the precipitation treatment and the sub-structure formation process by performing an initial precipitation treatment (i.e., annealing), followed by a lower subsequent rolling temperature to avoid precipitate-grain coarsening.

V. CONCLUSIONS

The following conclusions are drawn from this research:

1. The strength and ductility of a 2090 Al alloy are a strong function of the prior thermomechanical processing history of the material. Warm rolling 2090 Al alloy at rolling temperatures up to 450° C, however, produced only marginally superplastic response in the alloy.

2. The highest ductilities were achieved during tensile testing performed at 350° C. Testing 2090 Al alloy at temperatures above 350° C significantly lowered the elongations achieved regardless of the prior TMP used.

3. Warm rolling temperature and reheating time between rolling passes both affect the resultant strength and ductility. The highest ductility (320 percent) in subsequent tensile testing at 350° C was achieved with 450° C rolling combined with four-minute reheating between passes. The second highest ductility (236 percent) was achieved with 350° C rolling in concert with a reheating time between passes of 30 minutes. Both of these responses are in the superplastic range (above 200 percent).

4. Tensile testing at 300° C does show the material exhibiting the same trend as the Al-Mg alloy in the relationship between reheating interval between rolling passes and rolling temperature. At higher tensile testing temperatures, the ductility is enhanced by an increase in the rolling temperature for four-minute reheating times (resulting in a recovered structure). If a lower rolling temperature is utilized, the time between passes must be increased to achieve the same result.

5. The results obtained in this work do support the recovery model of continuous recrystallization, but the grain boundary structure produced is not sufficient for superplastic response to the extent obtained in the Al-Mg and Al-Mg-Li alloys.

VI. RECOMMENDATIONS

Recommendations for future research are:

1. Conduct the same series of experiments performed in this research, but utilize rolling temperatures higher than 450° C and shorten reheating times between passes to less than four minutes.

2. Perform tensile testing at 300° C and 350° C because the optimum results were obtained at those temperatures.

3. Conduct separate heat treatment (annealing) to initiate precipitation, followed by lower temperature rolling.

APPENDIX A

COMPUTER PROGRAM

```
REAL X,MR,SF,LOAD,AREA,ELONG,SENG,ENG,STRUE,ETRUE
INTEGER N,M

PRINT * , 'HOW MANY TIMES DO YOU WANT TO RUN THE PROGRAM ?'
READ * , M
DO 5 J = 1 , M
AREA = 0.0128
MR = 10.0
SF= .9357
PRINT *, 'ENTER X,LOAD'
READ * ,X,LOAD
ELONG = (X/MR)*SF
SENG = LOAD/AREA
ENG=ELONG /0.5
STRUE=SENG*(1+ENG)
ETRUE=LOG(1+ENG)
PRINT * , 'STRUE = ', STRUE
PRINT * , 'ETRUE = ', ETRUE
PRINT * , 'SENG = ', SENG
PRINT * , 'ENG = ', ENG
CONTINUE
STOP
END
```

APPENDIX B

TENSILE TEST DATA

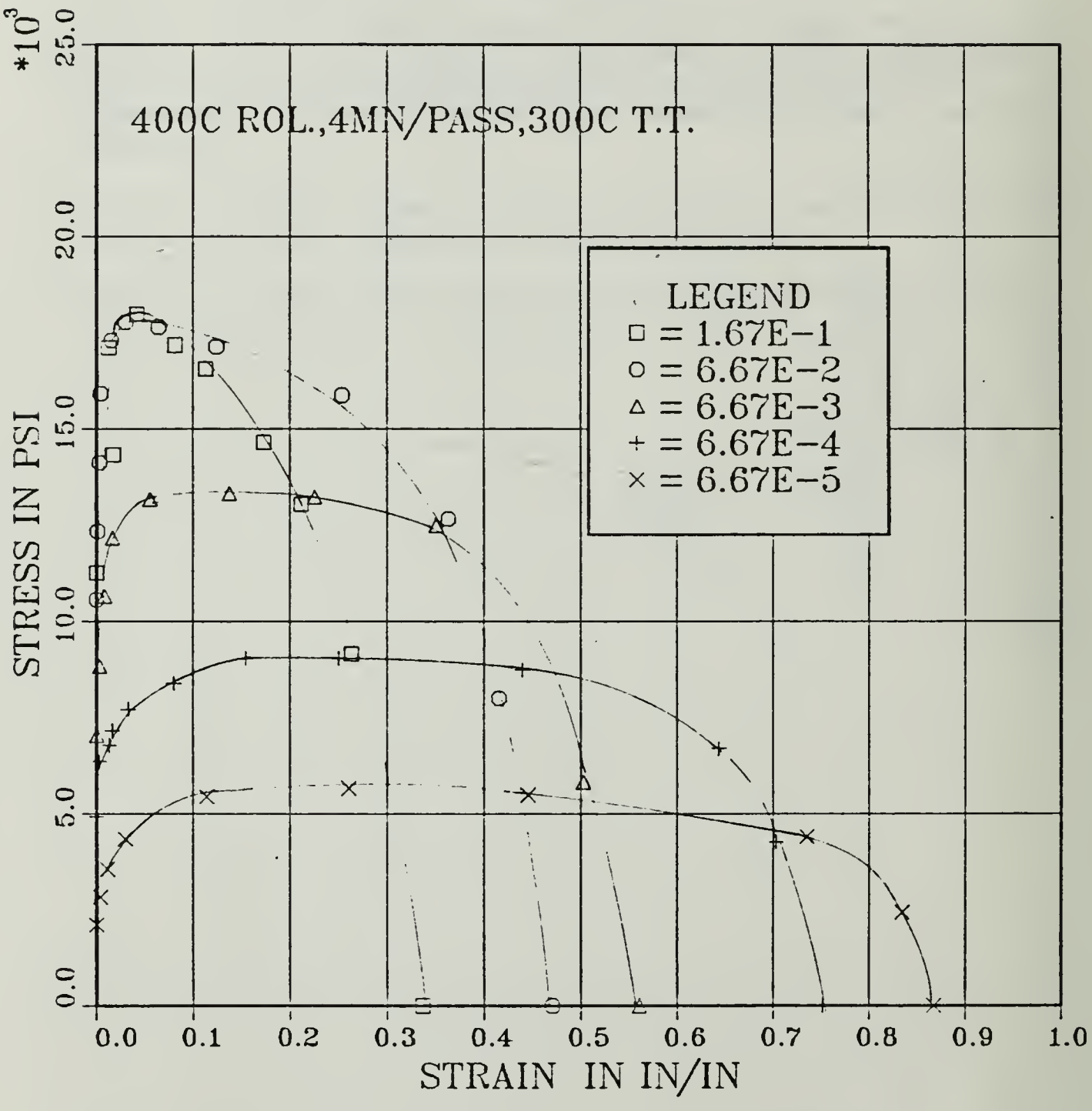

Figure B-1. **True Stress vs. True Strain for Tensile Testing Conducted at 300° C for Material Warm Rolled at 400° C With 4-Minute Reheating Time Between Rolling Passes**

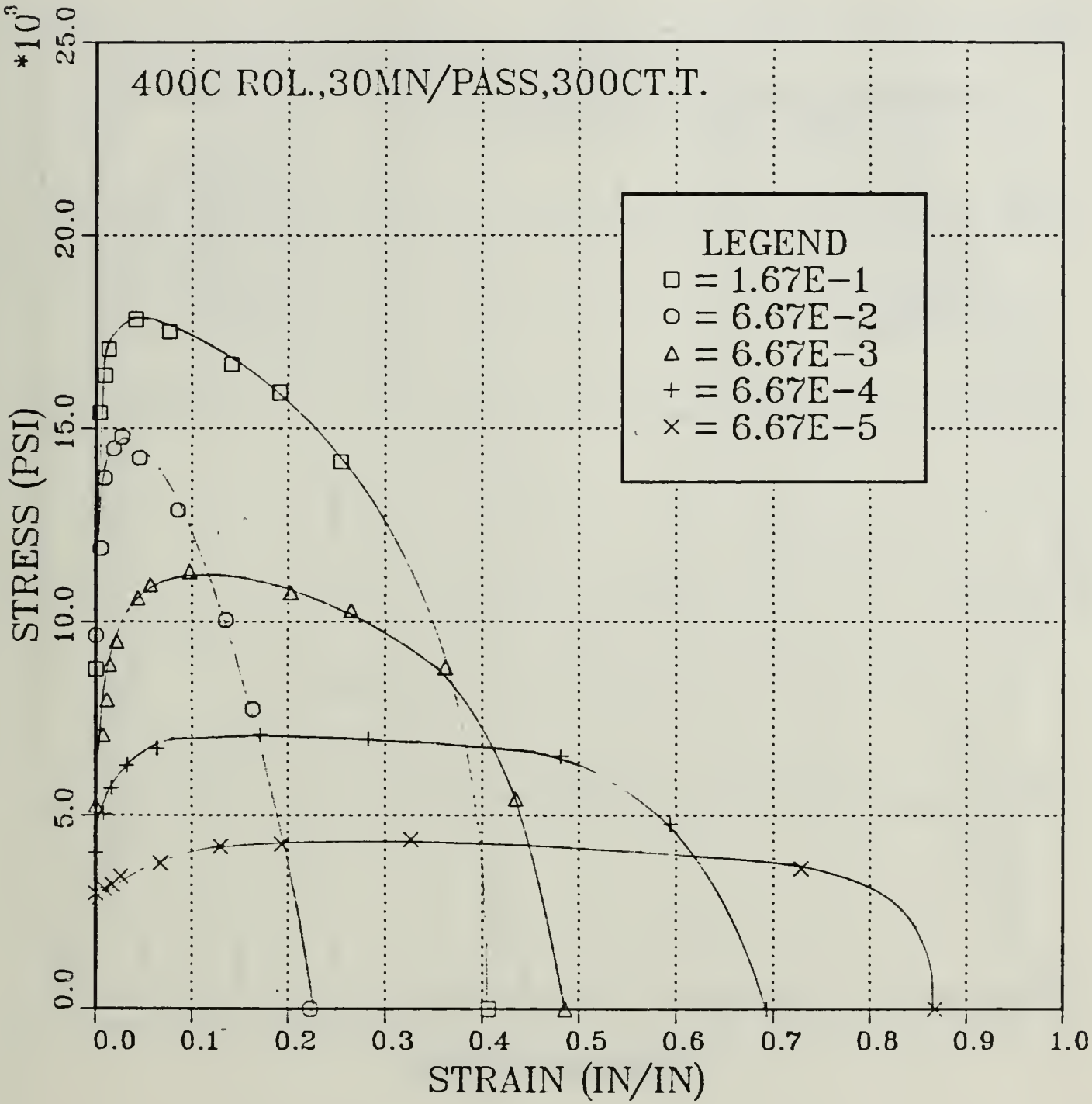

Figure B-2. **True Stress vs. True Strain for Tensile Testing Conducted at 300° C for Material Warm Rolled at 400° C With 30-Minute Reheating Time Between Rolling Passes**

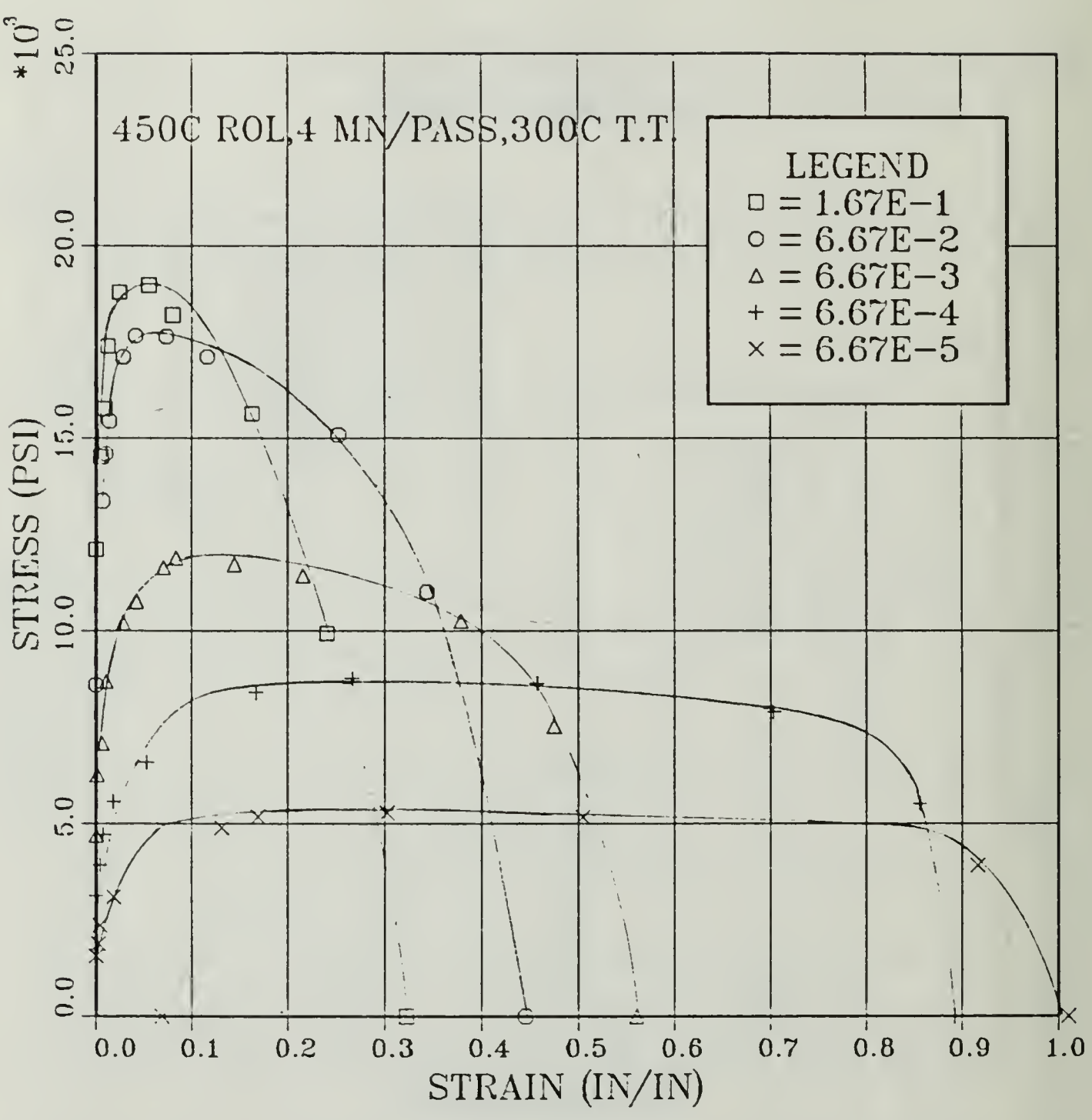

Figure B-3. **True Stress vs. True Strain for Tensile Testing Conducted at 300° C for Material Warm Rolled at 450° C With 4-Minute Reheating Time Between Rolling Passes**

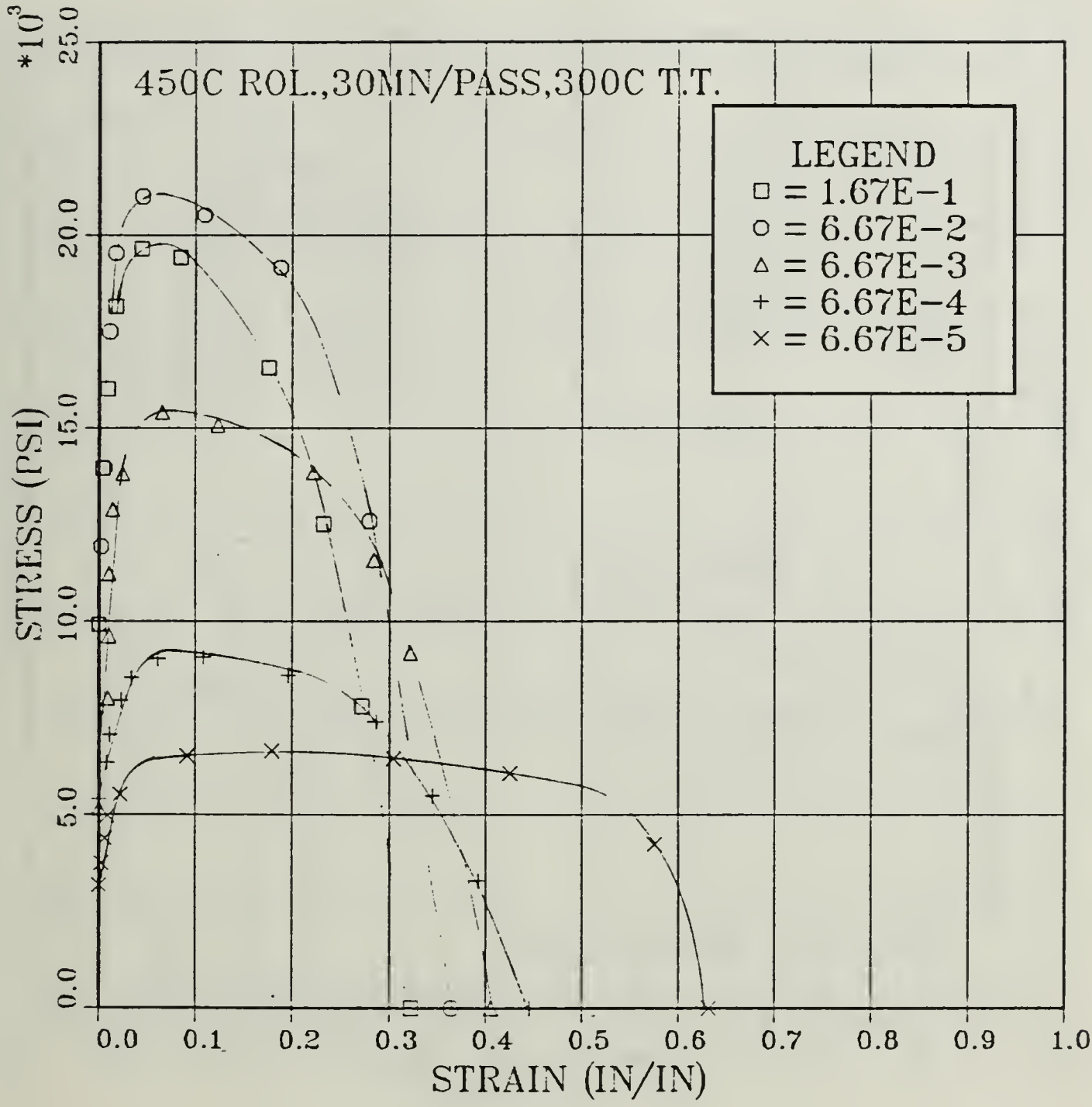

Figure B-4. **True Stress vs. True Strain for Tensile Testing Conducted at 300° C for Material Warm Rolled at 450° C With 30-Minute Reheating Time Between Rolling Passes**

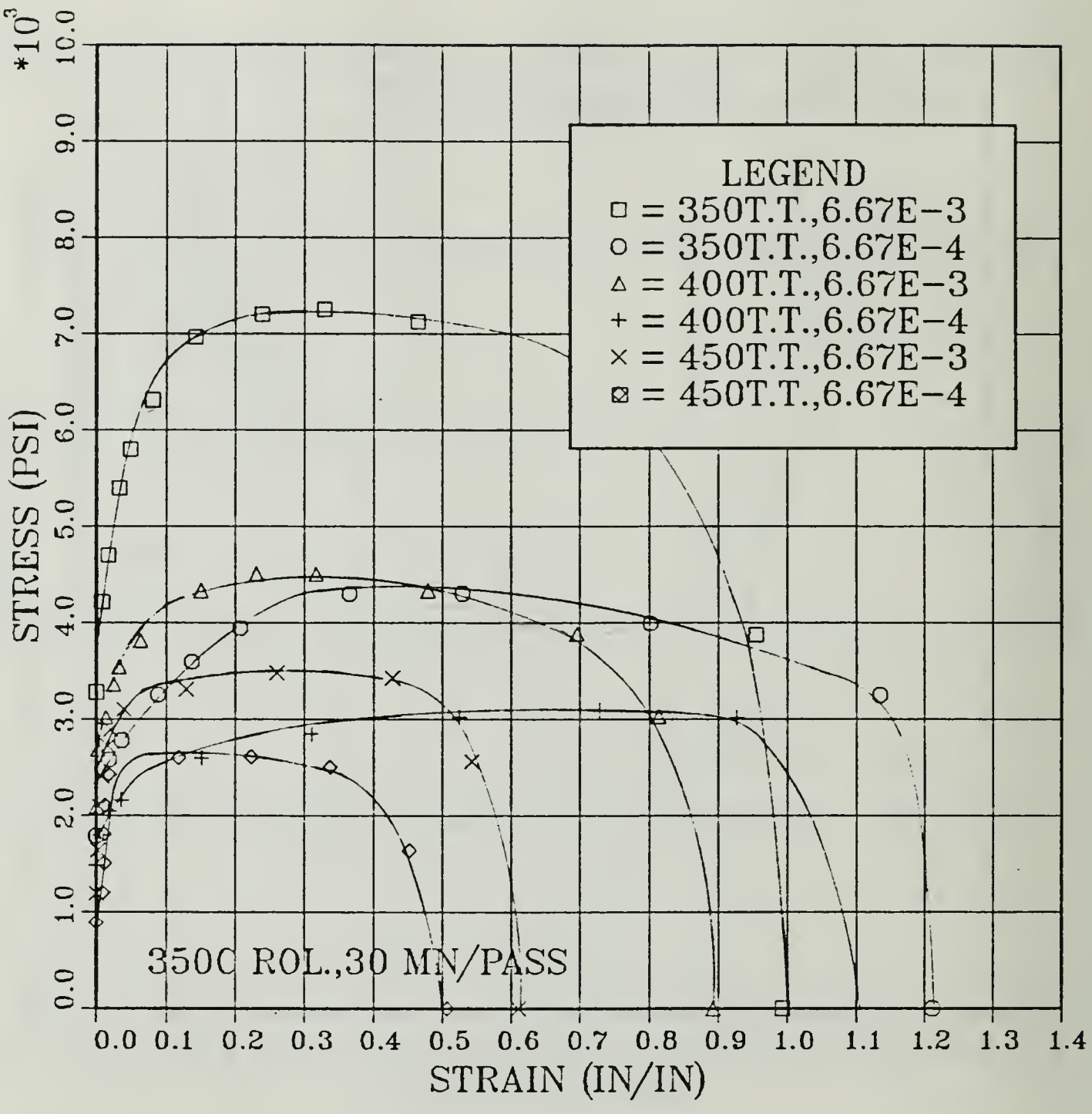

Figure B-5. **True Stress vs. True Strain for Tensile Testing Conducted as Shown in the Legend, for Material Processed at 350° C With 30-Minute Reheating Time Between Rolling Passes**

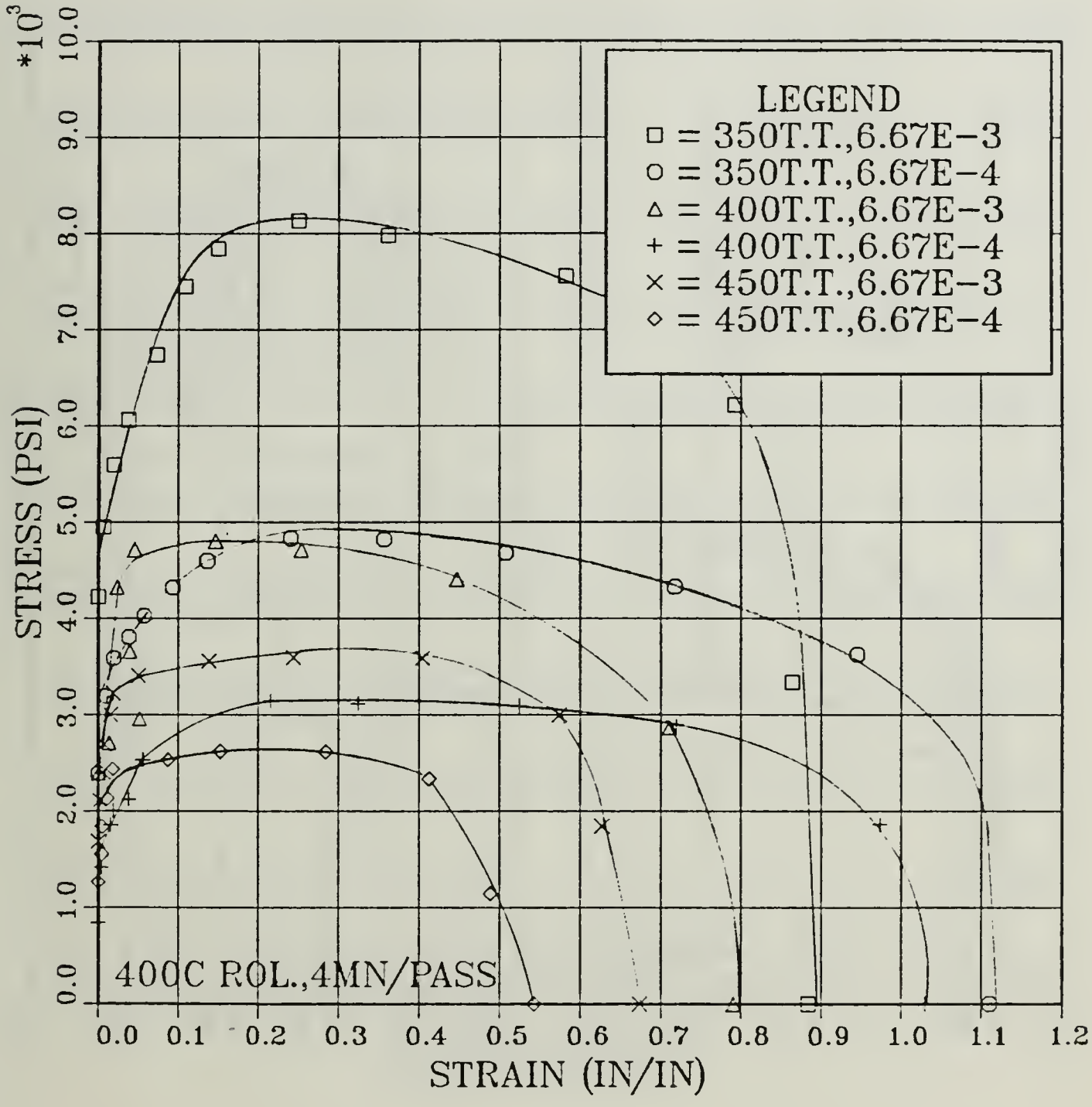

Figure B-6. **True Stress vs. True Strain for Tensile Testing Conducted as Shown in the Legend, for Material Warm Rolled at 400° C With 4-Minute Reheating Time Between Rolling Passes**

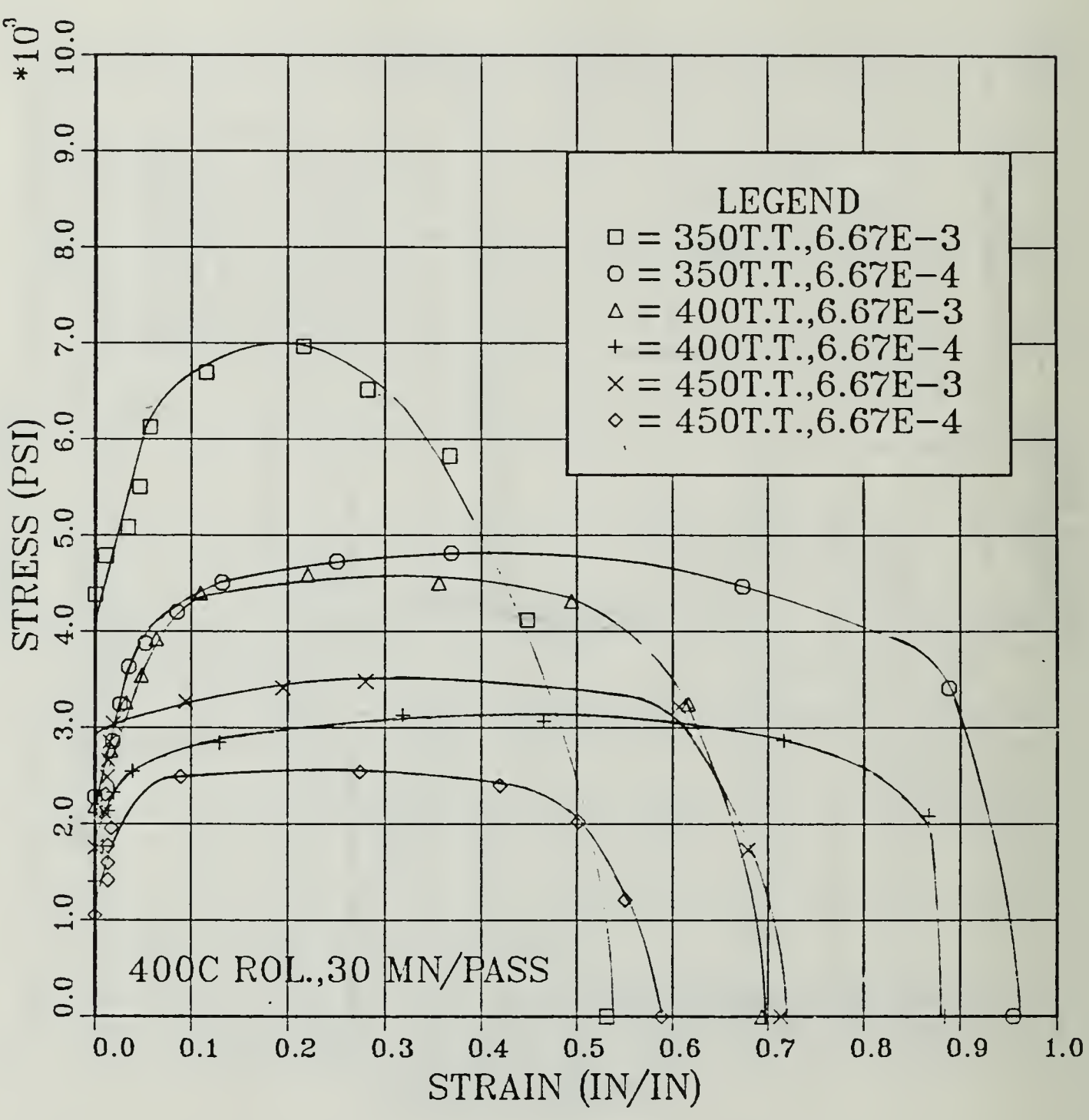

Figure B-7. **True Stress vs. True Strain for Tensile Testing Conducted as Shown in the Legend, for Material Warm Rolled at 400° C With 30-Minute Reheating Time Between Rolling Passes**

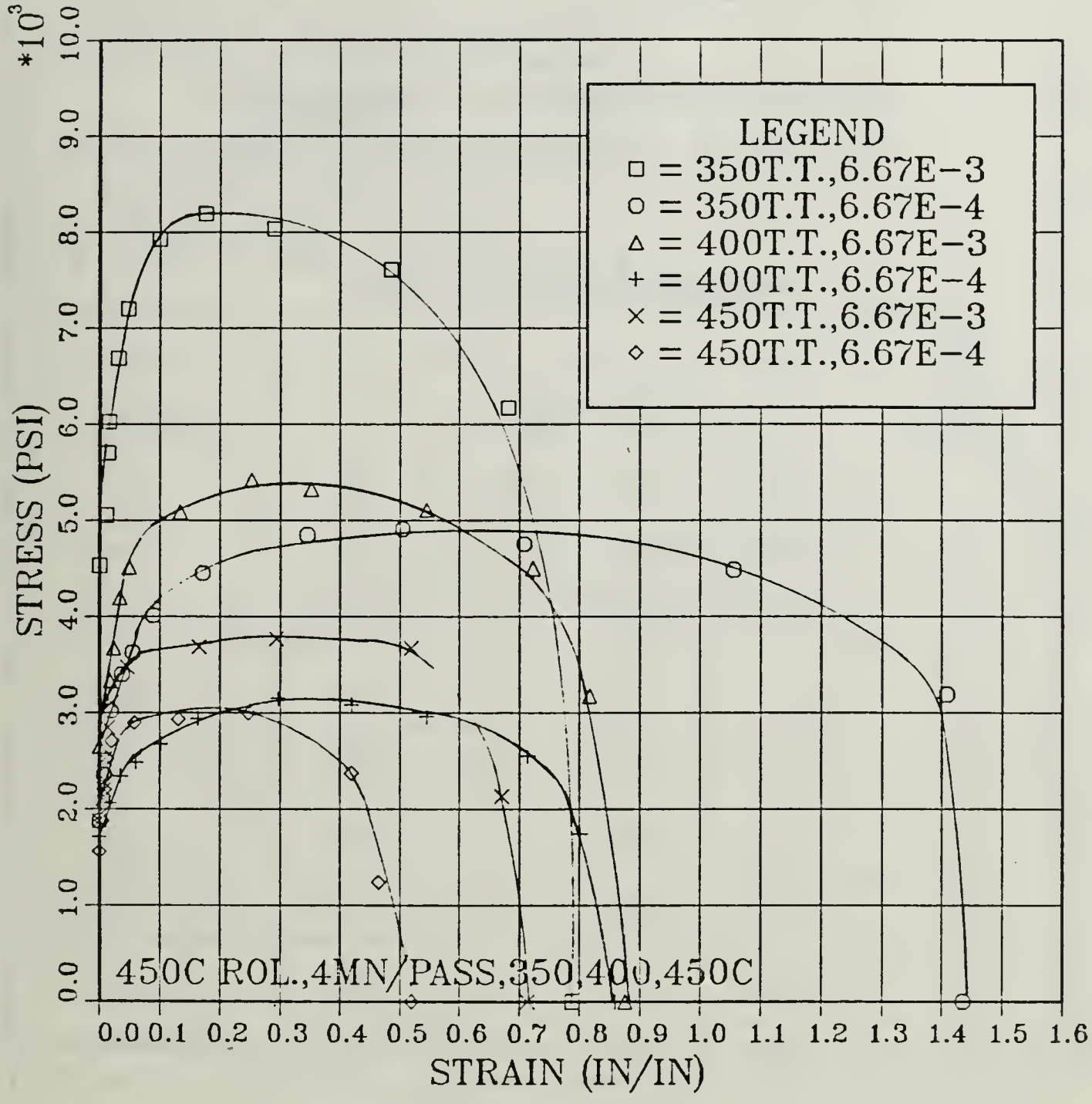

Figure B-8. **True Stress vs. True Strain for Tensile Testing Conducted as Shown in the Legend, for Material Processed at 450° C With 4-Minute Reheating Time Between Rolling Passes**

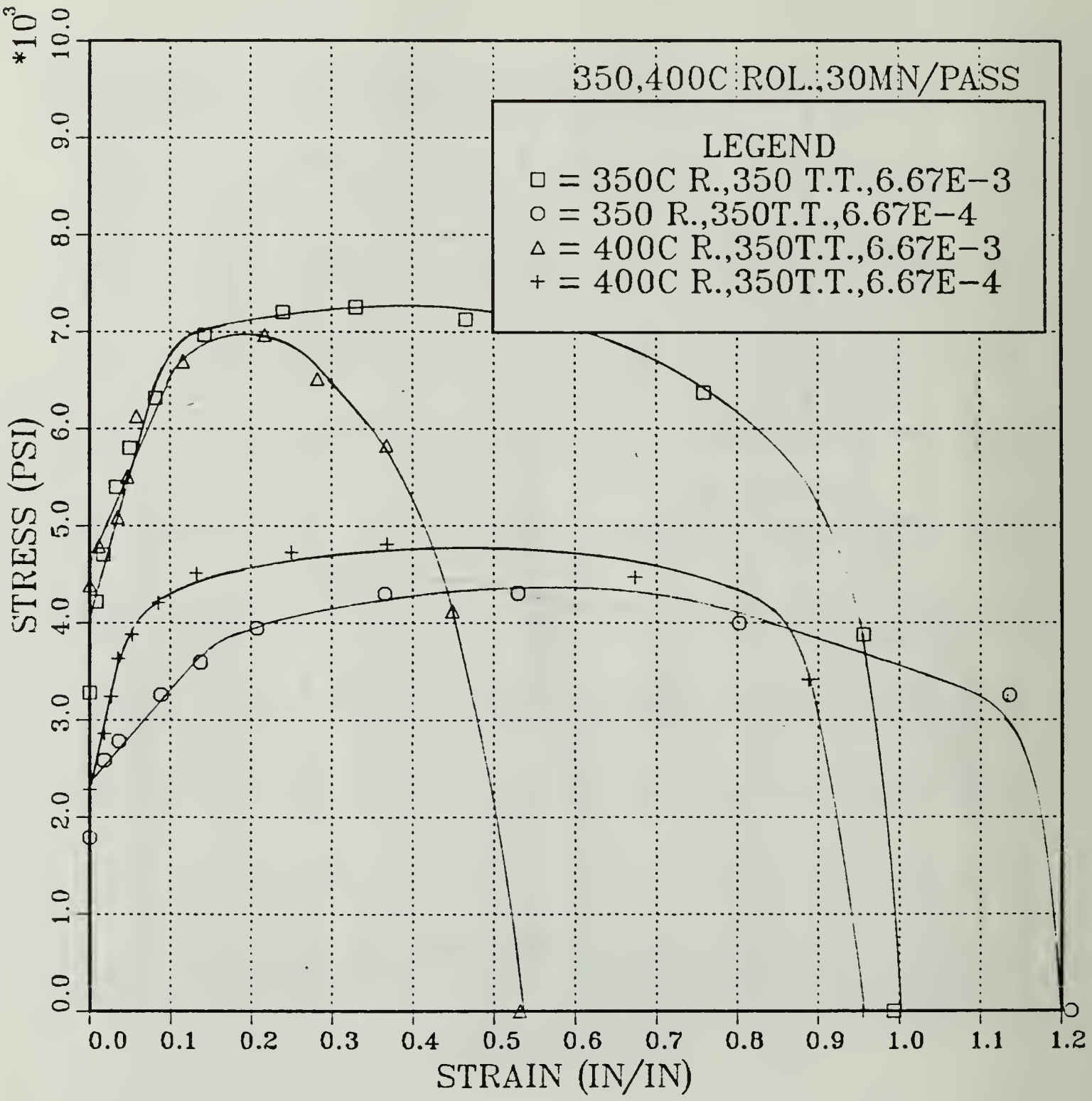

Figure B-9. **True Stress vs. True Strain for Tensile Testing Conducted at 350° C, for Material Warm Rolled at 350° and 400° C With 30-Minute Reheating Time Between Rolling Passes**

APPENDIX C

TRUE STRESS VS. STRAIN RATE DATA FOR STRAIN VALUES OF .02, .05, .10, AND .20

TABLE C-1

TENSILE TESTS AT 350° C

Process	Stress (PSI) at Strain Values of				Strain Rates (x6.67)
	.02	.05	.10	.20	
350° C 30 Min./Pass	4850	5800	6600	7200	10^{-3}
	2625	2975	3400	3975	10^{-4}
400° C 4 Min./Pass	5600	6375	7100	8100	10^{-3}
	3525	3900	4350	4775	10^{-4}
400° C 30 Min./Pass	4900	5775	6600	6925	10^{-3}
	3000	3800	4325	4700	10^{-4}
450° C 4 Min./Pass	6000	7250	7950	8200	10^{-3}
	3000	3600	4150	4550	10^{-4}

TABLE C-2

TENSILE TESTS AT 400° C

Process	Stress (PSI) at Strain Values of				Strain Rates (x6.67)
	.02	.05	.10	.20	
350° C 30 Min./Pass	3275	3750	4200	4450	10^{-3}
	2050	2250	2450	2650	10^{-4}
400° C 4 Min./Pass	4050	4650	4750	4800	10^{-3}
	2000	2375	2800	3075	10^{-4}
400° C 30 Min./Pass	2825	3600	4300	4600	10^{-3}
	2300	2625	2750	3000	10^{-4}
450° C 4 Min./Pass	3325	4500	4875	5325	10^{-3}
	2050	2450	2650	3025	10^{-4}

TABLE C-3

TENSILE TESTS AT 450° C

Process	Stress (PSI) at Strain Values of				Strain Rates (x6.67)
	.02	.05	.10	.20	
350° C 30 Min./Pass	2850	3225	3350	3400	10^{-3}
	2450	2500	2600	2640	10^{-4}
400° C 4 Min./Pass	3200	3350	3550	3625	10^{-3}
	2425	2500	2600	2650	10^{-4}
400° C 30 Min./Pass	3025	3150	3275	3400	10^{-3}
	2000	2300	2500	2505	10^{-4}
450° C 4 Min./Pass	3100	3400	3600	3725	10^{-3}
	2750	2850	2900	2975	10^{-4}

LIST OF REFERENCES

1. Spiropoulos, P. T., *Thermomechanical Processing of Al Alloy 2090 for Grain Refinement and Superplasticity*, M.S. Thesis, Naval Postgraduate School, Monterey, California, December 1987.

2. Mondolfo, L. F., *Aluminum Alloys: Structure and Properties*, Butterworth, 1976.

3. *Navy Times* article, p. 36, May 2, 1988.

4. Sherby, O. D., and Wadsworth, J., "Development and Characterization of Fine-Grain Superplastic Materials," *Deformation, Processing, and Structure*, pp. 354–384, 1987.

5. McNelley, T. R., and Hales, S. J., "Microstructural Evolution by Continuous Recrystallization in a Superplastic Al-Mg Alloy," *ACTA. Met.*, May 1988, Materials Engineering Group, Department of Mechanical Engineering, Naval Postgraduate School, Monterey, California.

6. Lloyd, D. J., and Moore, D. M., "Aluminum Alloy Design For Superplasticity," *Superplastic Forming of Structural Alloys*, Conference Proceedings of TMS–AIME and ASM 1982, N. E. Parton and C. H. Hamilton, eds., pp. 147–169, The Metalurgical Society of AIME, 1982.

7. Ferris, W. F., *The Age Hardening Response of Thermomechanical Processed Al-Mg-Li Alloys*, M.S. Thesis, Naval Postgraduate School, Monterey, California, December 1987.

8. Cotterill, P., and Mould, P. R., *Recrystallization and Grain Growth in Metals*, Surrey University Press, London, pp. 30–50, 1976.

9. McNelley, T. R., and Hales, S. J., "Continuous Recrystallization II: A Qualitative Model," to be published.

10. Humphreys, F. J., *The Nucleation of Recrystallization At Second Phase Particles In Deformed Aluminum*, ACTA. Met., vol. 25, pp. 1324–1344, 1977.

11. Hornbogen, N. E., *Combined Reactions*, Institute of Metals Lecture, The Metallurgical Society of Aime, 1979.

12. Sherby, O. D., and Burke, P. M., *Prog. Mat. Sci.*, vol. 13, p. 325, 1967.

13. Wise, J. E., "The Influence of Total Strain, Strain Rate and Reheating Time During Warm Rolling And The Superplastic Ductility of an Al-Mg-Zr Alloy," M.S. Thesis, Naval Postgraduate School, Monterey, California, March 1987.

14. Salama, A. A. A., "Analysis of Grain Refinement and Superplasticity in Aluminum-Magnesium Alloys," Ph.D. Dissertation, Naval Postgraduate School, Monterey Calfornia, December 1987.

15. McNelley, T. R., and Hales, S. J., "Continuous Recrystallization I: Experimental Evidence," to be published.

16. Nes, E., *Continuous Recrystallization And Grain Growth During Superplastic Flow*, Division of Physical Metallurgy, The Norwegian Institute of Technology, University of Trondheim, Superplasticity, International Conference on Superplasticity, Sept 1985, Grenoble France.

17. *Annual Book of ASTM Standards*, vol. 02.02, pp. 1044–1055, American Society for Testing and Materials, 1986.

18. *Source Book on Selection and Fabrication of Aluminum Alloys*, American Society for Metals, 1978.

19. Anamet Laboratories, Inc., Hayward, California, Laboratory Report No. 887.180, 25 August 1987.

20. McNelley, T. R., Lee, E. W., and Garg, A., "Superplasticity in Thermomechanically Processed High-Mg, Al-Mg-X Alloys," *Aluminum Alloys, Their Physical and Mechanical Properties*, vol. II, Conference Proceedings, Engineering Materials Advisory Services, Ltd., 1986.

21. Kuhnert, G. J., *The Influence of Warm Rolling Parameters (Temperature and Reheating Time Between Passes) On The Superplastic Responses of Al-Mg Alloys*, M.S. Thesis, Naval Postgraduate School, Monterey, California, June 1988.

22. Yoshida, H., and coworkers, "The Effect of Grain Boundary Precipitation on the Superplasticity of Al-Li Alloys," 4th International Al-Li Conference in Paris, France, 10–12 June 1987.

INITIAL DISTRIBUTION LIST

		No. Copies
1.	Defense Technical Information Center Cameron Station Alexandria, VA 22304–6145	2
2.	Library, Code 0142 Naval Postgraduate School Monterey, CA 93943-5002	2
3.	Department Chairman, Code 69Hy Department of Mechanical Engineering Naval Postgraduate School Monterey, CA 93943-5000	1
4.	Professor T. R. McNelley, Code 69Mc Department of Mechanical Engineering Naval Postgraduate School Monterey, CA 93943-5000	5
5.	Dr. S. J. Hales, Code 69He Department of Mechanical Engineering Naval Postgraduate School Monterey, CA 93943-5000	1
6.	Naval Air Systems Command, Code AIR 931 Naval Air Systems Command Headquarters Washington, DC 20361	1
7.	Dr. Eui-Whee Lee, Code 6063 Naval Air Development Center Warminster, PA 18974	1
8.	LCDR Gary E. Groh Department of Mechanical Engineering Naval Postgraduate School Monterey, CA 93943-5000	1
9.	LT Henry C. Regis 685 Greenwood Avenue Fairhope, AL 36532	1

Thesis
R2881 Regis
c.1 Processing of 2090
aluminum alloy for super-
plasticity.